HHS Public Access

Author manuscript

J Med Chem. Author manuscript; available in PMC 2021 April 06.

Published in final edited form as:

J Med Chem. 2021 January 14; 64(1): 279–297. doi:10.1021/acs.jmedchem.0c01664.

Small Molecule Inhibitors Targeting Biosynthesis of Ceramide, the Central Hub of the Sphingolipid Network

Jan Skácel,
Johns Hopkins Drug Discovery and Department of Neurology, Johns Hopkins University, Baltimore, Maryland 21205, United States

Barbara S. Slusher,
Johns Hopkins Drug Discovery and Department of Neurology, Johns Hopkins University, Baltimore, Maryland 21205, United States

Takashi Tsukamoto*
Johns Hopkins Drug Discovery and Department of Neurology, Johns Hopkins University, Baltimore, Maryland 21205, United States

Abstract

Ceramides are composed of a sphingosine and a single fatty acid connected by an amide linkage. As one of the major classes of biologically active lipids, ceramides and their upstream and downstream metabolites have been implicated in several pathological conditions including cancer, neurodegeneration, diabetes, microbial pathogenesis, obesity, and inflammation. Consequently, tremendous efforts have been devoted to deciphering the dynamics of metabolic pathways involved in ceramide biosynthesis. Given that several distinct enzymes can produce ceramide, different enzyme targets have been pursued depending on the underlying disease mechanism. The main objective of this review is to provide a comprehensive overview of small molecule inhibitors reported to date for each of these ceramide-producing enzymes from a medicinal chemistry perspective.

Graphical Abstract

*Corresponding Author Takashi Tsukamoto − *Johns Hopkins Drug Discovery and Department of Neurology, Johns Hopkins University, Baltimore, Maryland 21205, United States;* Phone: (410) 614-0982; ttsukamoto@jhmi.edu; Fax: (410) 614-0659.

Complete contact information is available at: https://pubs.acs.org/10.1021/acs.jmedchem.0c01664

The authors declare no competing financial interest.

DEDICATION

Dedicated to Dr. Camilo Rojas in recognition of his outstanding contributions to the field of drug discovery research throughout his industrial and academic career on the occasion of his retirement from Johns Hopkins University.

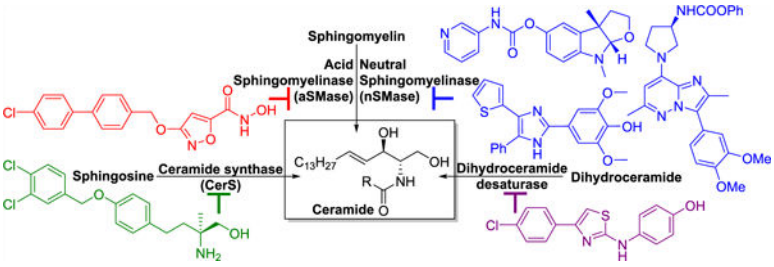

1. INTRODUCTION

Sphingolipids belong to a class of non-glycerol-based lipids built on a sphingosine backbone. Sphingosine derivatives acylated at the amino group with fatty acids of different chain length and degree of unsaturation are termed ceramides. Because of the structural variation in the fatty acid component, ceramides can occur in several structurally different forms. For instance, ceramide formed from sphingosine (d18:1) and oleic acid (18:1(9Z)) containing a total of 18 carbons and a C8–C9 Z-double bond is referred to as Cer(d18:1/18:1(9Z)).[1] Cumulative evidence suggests that different ceramides, in terms of the fatty acid composition, may play distinct and tissue-specific physiological roles under various biological contexts.[2]

Ceramides are known to be synthesized through three major pathways, namely, the de novo biosynthesis pathway, the salvage pathway, and sphingomyelin hydrolysis (Figure 1).[3,4] Because of their pathophysiological implications in diseases, some of the enzymes involved in these pathways have been extensively studied as therapeutic targets including ceramide synthase, dihydroceramide desaturase, and sphingomyelinase, each of which catalyzes the final step in the de novo biosynthesis pathway, the salvage pathway, and sphingomyelin hydrolysis, respectively. Other ceramide-producing enzymes include glucocerebrosidase, galactocerebrosidase, and ceramide-1-phosphate phosphatase. With the increasing interest in ceramide biosynthesis as therapeutic targets, there are a number of well-written review articles detailing the biological and physiological aspects of these ceramide-producing enzymes.[5–16] There are also review articles on small molecule inhibitors of these enzymes, [17–21] though they are relatively limited in scope and lack detailed insights from a medicinal chemistry perspective. This Perspective provides a comprehensive and in-depth overview of small molecule inhibitors reported to date for each of these ceramide-producing enzymes including the latest development in this field with greater potential for therapeutic application.

2. DIHYDROCERAMIDE DESATURASE

De novo synthesis of ceramide begins with decarboxylative condensation of L-serine and palmitoyl-CoA catalyzed by serine C-palmitoyltransferase. The resulting product, 3-dehydrosphinganine, is converted into sphinganine by 3-dehydrosphinganine reductase. Ceramide synthase catalyzes the acylation of sphinganine with fatty-acyl-CoAs of varying chain length to yield dihydroceramides. In the final step of the de novo biosynthesis pathway, dihydroceramide desaturase converts dihydroceramides into ceramides. While

dihydroceramide desaturase 1 (DES1) encoded by DEGS1 in human displays only desaturase activity, its closest paralog, dihydroceramide desaturase 2 (DES2) encoded by DEGS2, exhibits both desaturase and hydroxylase activities. DEGS1 deficiency has recently been reported to lead to an imbalance between saturated/unsaturated sphingolipids and cause leukodystrophy and peripheral hypomyelination,[22] highlighting the clinical significance of DES1. DES1 has been also implicated as a therapeutic target in various diseases including cancer,[23] Alzheimer's disease,[24] and diabetes.[25] Along with these findings, a number of structurally diverse DES1 inhibitors have been reported in the literature.[21]

GT11 (**1**) is one of the first DES1 inhibitors described in the literature (Figure 2).[26] It is a ceramide derivative in which the C4–C5 double bond of the sphingosine component is replaced by a cyclopropene moiety. The design of this molecule was based on early reports on the activity of sterculic acid as a potent inhibitor of the **Δ9**-stearoyl-CoA desaturase.[27] As expected from its structure, kinetics studies using rat liver microsomes revealed that GT11 (**1**) inhibits DES1 in a competitive manner with respect to *N*-octanoylsphinganine with a K_i value of 6 μM.[28] Interestingly, GT11 (**1**) was found to inhibit dihydroceramide desaturase activity in primary cultured cerebellar neurons with an approximately 250-fold greater inhibitory potency, presumably due to a local subcellular enrichment of the inhibitor in the endoplasmic reticulum, the main site of action of the enzyme.[29] It should be noted, however, that GT11 (**1**) was also reported to display greater potency when HGC27 cell lysates were used as a source of the enzyme with an IC_{50} value of 52 nM and a K_i value of 22 nM.[30]

XM462 (**2**) is a mechanism-based DES1 inhibitor in which the C5 methylene group of the sphinganine component is replaced by a sulfur atom (Figure 2).[31] It inhibits desaturase activity in rat liver microsomes with an IC_{50} value of 8.2 μM. The rationale for incorporating a sulfur atom into the sphinganine component is based on the previous reports on the activity of some thia fatty acids as fatty acyl-CoA desaturase inhibitors.[32,33] XM462 (**2**) was found to be a mixed-type inhibitor with K_{iapp} and α values of 2 μM and 0.83, respectively. Although the precise mechanism of inhibition was not investigated, the ceramide analog is anticipated to bind to the enzyme active site, where its C4 hydrogen is removed as a radical to afford the carbon radical intermediate in equilibrium with the sulfur radical species. The inhibition may then arise from coordination of the intermediate(s) to the enzyme active site.

There are several other ceramide analogs reported as DES1 inhibitors including those derived from GT11 (**1**)[28,34] and XM462 (**2**).[35] Most notably, ceramide analog **3** (Figure 2) containing a C6–C7 double bond was found to act as a potent DES1 inhibitor with an IC_{50} value of 155 nM when HGC27 cell lysates were used as a source of the enzyme.[30] Contrary to expectations based on its structural similarity to DES1 substrates, compound **3** showed a noncompetitive type of inhibition.

Fenretinide (**4**), also known as *N*-(4-hydroxyphenyl)-retinamide (4-HPR), is a synthetic retinoid derivative originally developed as a chemotherapeutic agent because of its ability to attenuate cancer cell growth with relatively low toxicity (Figure 3).[36] Fenretinide (**4**) was first recognized as a DES1 inhibitor when it was found to increase dihydroceramides in a dose dependent manner in SMS-KCNR cells.[37] Subsequently, DES1 was confirmed as the primary target for fenretinide (**4**) using rat liver microsomes with an IC_{50} value of 2.32 μM.

[38] In 20 min incubation experiments, fenretinide (**4**) acted as a competitive inhibitor with a K_i value of 8.28 μM. In addition to fenretinide (**4**), its known metabolites were evaluated for their ability to inhibit desaturase activity. Among them, 4-oxo-*N*-(4-hydroxyphenyl)retinamide **5** (4-oxo-4-HPR, Figure 3) showed the highest inhibitory potency with an IC_{50} value of 1.68 μM. *N*-(4-Methoxyphenyl)retinamide **6** (4-MPR) and 4-oxo-*N*-(4-methoxyphenyl)retinamide **7** (4-oxo-4-MPR) had minimal effects on DES1 activity (Figure 3), demonstrating the essential role played by the phenolic moiety in the potent inhibitory activity.

SKI II (**8**) is an orally available dual inhibitor of sphingosine kinases 1 (SK1) and 2 (SK2) with K_i values of 16 μM and 7.9 μM, respectively (Figure 4).[39,40] It was later discovered that SKI II (**8**) also inhibits DES1.[41] Unlike fenretinide (**4**), SKI II (**8**) was found to act as a noncompetitive inhibitor of DES1 in HGC-27 cell lysates with a K_i value of 0.3 μM despite that they share the 4-aminophenol moiety. On the basis of these findings, it is speculated that SKI II (**8**) targets the upstream enzyme, cytochrome b5 reductase (Cb5R), which plays an essential role in the desaturation process by regenerating ferrocytochrome b5. Compounds **9** and **10** (Figure 4), analogs of SKI II (**8**), were also reported as inhibitors of desaturase activity in Jurkat cells with varying degrees of inhibitory potency and selectivity for SK1 and SK2,[42] which should, together with other SKI II (**8**) analogs devoid of desaturase inhibitory activity, serve as useful probes to understand the biology of SK1, SK2, and DES1.

More recently, a series of DES1 inhibitors containing a 4-acylaminophenol or 6-acylamino-3-pyridinol scaffold were disclosed in a patent application (Figure 5).[43] Compounds **11** and **12** were reported to potently inhibit DES1 activity in Jurkat cells with an IC_{50} value of 1 nM, while fenretinide (**4**), used as a control, exhibited an IC_{50} value of 100–250 nM under the same assay conditions. The impact of converting a phenol to a 3-pyridinol moiety was most profound for compound **13**, which exhibited >20-fold improvement in potency over the corresponding phenol derivative 14 possessing the same acyl group. At present, only limited pharmacological data are available for these highly potent DES1 inhibitors. It remains to be seen whether these compounds have the potential to be developed into viable therapeutic agents.

There are other non-ceramide analogs reported as DES1 inhibitors including resveratrol, celecoxib, curcumin, and **Δ9**-tetrahydrocannabinol (THC).[21] Their utility as DES1 inhibitors, however, remains questionable given their rather weak inhibitory activity against DES1 coupled with the fact that they act on other targets more potently and/or display polypharmacological behaviors.

3. CERAMIDE SYNTHASE

Ceramide synthase (CerS) catalyzes the acylation of sphingoid bases with fatty-acyl-CoAs of varying chain length.[44] As mentioned earlier, CerS can recognize sphinganine as a substrate and produce dihydroceramides, penultimate intermediates of the de novo biosynthesis pathway. CerS can also directly produce ceramides when sphingosine is used as a substrate via the salvage pathway, reutilizing sphingosine formed as a result of degradation of higher order sphingolipids. CerS is encoded by six distinct genes (CerS1–6), each of

which shows preference for a particular range of Acyl-CoA substrates (Figure 6).[10,44,45] For instance, CerS1, which is primarily expressed in the brain, has a high substrate preference for stearoyl-CoA. Indeed, C18-ceramide was reported to be the most abundant ceramide in the rat brain, representing nearly half of the total ceramide amount.[46] Given the distinct substrate specificity and tissue distribution shown by each of the six isoforms, it is not surprising that the clinical and pathological significance of CerS varies among them.[9,10,47] Therefore, the therapeutic potential of CerS inhibition highly depends on the ability to target a specific isoform of CerS. Until recently, though, there had been no isoform-selective CerS inhibitors, hindering efforts to develop CerS-targeting therapeutic agents.

Fumonisin B1 (**15**) (Figure 7), a mycotoxin produced by *Fusarium moniliforme*, is one of the first reported CerS inhibitors.[48] In rat liver microsomes, fumonisin B1 (**15**) was found to inhibit conversion of [^{3}H]sphingosine to [^{3}H]ceramide with an IC_{50} value of 0.1 μM. It is postulated that the two tricarballylic acid side chains of fumonisin B1 (**15**) play a crucial role in interacting with the acyl-CoA binding site while its amino group mimics that of sphinganine/sphingosine.[49] Inhibition kinetics studies using mouse brain microsomes indicated that fumonisin B1 (**15**) is a competitive inhibitor with respect to sphinganine while it displayed a mixed-type inhibition with respect to stearoyl-CoA.[50] Although speculative, it is conceivable that a fraction of fumonisin B1 (**15**) was hydrolyzed in brain microsomes to form aminopentol (**16**) (Figure 7), which is known to serve as a CerS substrate by making the fatty acyl-CoA binding site accessible to an acyl donor.[51] This may explain the observed mixed-type inhibition with respect to stearoyl-CoA by fumonisin B1 (**15**). It should also be noted that the resulting *N*-acyl derivatives of aminopentol likely serve as CerS inhibitors as seen with *N*-palmitoyl and *N*-nervonoyl derivatives of aminopentol.[51,52]

Fumonisin B1 (**15**) has been widely used to study effects of CerS inhibition on the sphingolipid metabolism and cell viability.[9,10] Fumonisin B1 (**15**) is cytotoxic to various mammalian cell lines, at least in part due to its lack of isoform selectivity.[53] This has hindered efforts to assess the therapeutic potential of selectively targeting each isoform.

FTY720 (**17**), also known as fingolimod, is a sphingosine-like molecule approved by FDA for the treatment of the relapsing form of multiple sclerosis (Figure 8). After enantiospecific monophosphorylation, the resulting metabolite **18** acts as a functional antagonist of sphingosine-1-phosphate (S1P) receptors *in vivo*. Interestingly, FTY720 (**17**) itself was found to inhibit N-acylation of dihydrosphingosine with docosanoyl-CoA with an IC_{50} value of 6.4 μM in the human pulmonary artery endothelial cell (HPAEC) lysate.[54] It appears to act as a competitive inhibitor with respect to dihydrosphingosine with a K_i value of 2.15 μM for CerS2 when C22-CoA was used as an acyl donor. A different research group, however, reported more complex inhibition kinetics of FTY720 (**17**) using homogenates prepared from HEK cells overexpressing CerS4, namely, noncompetitive and uncompetitive inhibition toward C18-CoA and sphinganine, respectively.[55] Yet another group showed that FTY720 (**17**) is competitive with respect to fluorescent NBD-sphinganine and noncompetitive with respect to C16:0-CoA.[56]

The (*R*)- and (*S*)-enantiomers of 2-amino-4-(4-heptylox-yphenyl)-2-methylbutanol (AAL) are derivatives of FTY720 (**17**) in which the benzylic carbon was replaced by an ether

oxygen and one of the two prochiral hydroxymethyl groups is replaced by a methyl group (Figure 8).[57] It was reported that (*R*)-AAL (**19**) but not (*S*)-AAL (**20**) is phosphorylated by recombinant mouse sphingosine kinase 1a.[57] This finding is consistent with the enantiospecificity of sphingosine kinases displayed toward FTY720 (**17**). Interestingly, the nonphosphorylatable enantiomer (*S*)-AAL (**20**) was subsequently found to inhibit C16:0 CerS activity of HEK293 lysates (~50% inhibition at 10 μM) in a competitive manner with respect to NBD-sphinganine.[56] None of the three additional analogs **21–23** (Figure 8) showed substantial CerS inhibitory activity at 10 μM, suggesting that both the amino group and the long carbon chain of (*S*)-AAL (**20**) are essential for the potent inhibitory activity.[56]

Investigation on the isoform selectivity of (*S*)-AAL (**20**) revealed that it inhibits CerS1 potently (>90% inhibition at 10 μM) and, to a lesser extent, CerS5 and CerS6 (nearly 50% inhibition at 10 μM).[58] Although benzyloxy analog **24** (Figure 8) was found to be a somewhat weaker CerS1 inhibitor (76% inhibition at 10 μM), it showed no inhibitory activity toward CerS2 and CerS4–6, representing one of the first isoform-selective CerS inhibitors. It should be noted that (*S*)-AAL (**20**) and compound **24** (at 10 μM) have CerS1 inhibitory activity–cytotoxicity ratios of 0.2 and 3.6, respectively. The results suggest the possibility of differentiating CerS1 inhibitory activity from cytotoxicity, an important step forward for the future therapeutic development of CerS inhibitors.

In another study, *N*-alkyl and *N*-acyl derivatives **25–28** (Figure 9) were profiled for their effects on ceramide synthase activity of cell lysates and live cells by measuring the levels of C14–C24 ceramides or dihydroceramides.[59] For instance, compounds **25** inhibited C16-, C18-, and C24-dihyroceramide synthesis with IC_{50} values of 25.7, 50.7, and 60.6 μM, respectively, in a microsomal fraction of HCT-116 cells. Subsequent experiments using a cell lysate of CerS2, CerS4, or CerS6 overexpressing HT-116 cells indicated that compound **25** preferentially inhibits CerS2 and CerS4.

More recently, P053 (**29**), a dichloro analog of **24**, was reported as a potent and selective inhibitor of CerS1 (Figure 9).[60] P053 (**29**) inhibited human and murine CerS1 (hCerS1 and mCerS1) with IC_{50} values of 0.54 and 0.46 μM, respectively, while it showed substantially lower inhibitory potency against hCerS2, mCerS2, hCerS4, mCerS5, and hCerS6 (IC_{50} = 7–30 μM). The inhibition of CerS1 by P053 (**29**) appears to be noncompetitive with respect to either sphinganine or C18 fatty acyl-CoA. Consistent with its *in vitro* isoform selectivity, P053 (**29**) selectively reduced C18 ceramide and other C18 sphingolipids in HEK293 cell culture. P053 (**29**) is orally available in mice and reduced C18 ceramide levels in skeletal muscles of mice on a high-fat diet, leading to the enhancement of fatty acid oxidation and reduction in overall adiposity. These findings demonstrate the therapeutic potential of CerS1 inhibition for the treatment of obesity.

4. SPHINGOMYELINASE

Sphingomyelin, the most abundant form of sphingolipids, is a non-glycerol-based phospholipid in which the primary alcohol of ceramide is linked to choline through a phosphodiester bond.[61,62] Sphingomyelin is synthesized from ceramide by sphingomyelin synthase in the Golgi apparatus. Because of varying chain length (C14 to C26) of the fatty

acid moiety of the ceramide molecule, sphingomyelin occurs in a number of structurally different forms. Upon synthesis, sphingomyelin is exported to other membrane systems. Indeed, sphingomyelin constitutes a significant fraction of the total lipid composition of the plasma and lysosomal membranes.[63] Membrane sphingomyelin can be hydrolyzed back to ceramide via hydrolysis of the phosphodiester catalyzed by sphingomyelinase, thereby serving as a reservoir for ceramide.[64] Sphingomyelinase can be divided into three evolutionarily unrelated classes based on their pH optima: acid sphingomyelinase (aSMase), neutral sphingomyelinase (nSMase), and alkaline sphingomyelinase. No potent inhibitors have been reported for alkaline sphingomyelinase to date, and thus this topic will not be covered in this review. On the other hand, tremendous efforts have been made to identify potent inhibitors of aSMase and nSMase, in part driven by the therapeutic potential of targeting these enzymes for the treatment of various diseases, including cancer, neurodegenerative diseases, major depression disorder, pulmonary inflammation, atherosclerosis, and viral infections.

4.1. Acid Sphingomyelinase.

Two forms of aSMase, both encoded by the SPMD1 gene, have been known to exist as a result of two distinct post-translational trafficking pathways within the ER-Golgi network.[13] Lysosomal aSMase is transported to the endolysosomal compartment and anchored to the inner lysosomal membrane. Secretory aSMase is transported to the outer leaflet of the plasma membrane and secreted into the extracellular space under certain conditions.

Clinical significance of aSMase has been well recognized as some forms of Niemann–Pick disease, a lysosomal storage disorder, were found to be caused by loss-of-function mutations in the SMPD1 gene.[65] Upregulation of aSMase has also been implicated in a number of diseases including several neurodegenerative disorders where excess ceramide is believed to play a pathogenic role.[12] As described later, these findings have spurred efforts to develop aSMase inhibitors as therapeutic agents.

Several crystal structures have been reported for mammalian aSMase.[66–68] Two distinct conformations were observed in the crystal structures of murine aSMase depending on the folding and positioning of the membrane-interacting N-terminal saposin domain.[66] A closed globular conformation (PDB code 5FI9) is believed to be predominant in the absence of membranes and render the enzyme inactive (Figure 10A), while an open conformation (PDB code 5FIB) is expected to establish an interface with the catalytic domain essential for activity (Figure 10B). The active site carries a binuclear zinc complex, playing a central role in the catalytic process at the core of the active site. A hydrophobic track that extends from the edge of the active site to the saposin domain is predicted to accommodate the fatty acid chains of sphingomyelin. aSMase is positively charged at acidic lysosomal pH and is tightly associated with lysosomal membrane surfaces, presumably through the positively charged residues in the saposin domain. This formed the mechanistic basis for indirect inhibition of aSMase by cationic amphiphilic molecules, which constitute one of the two major classes of aSMase inhibitors, the other being those directly interacting with the enzyme.

AY-9944 (**30**) (Figure 11), originally reported as an inhibitor of cholesterol biosynthesis,[69] was later found to recapitulate the pathological features similar to those found in Niemann–

Pick disease in rats.[70] Furthermore, it was found that aSMase activity was significantly reduced in the tissues of rats treated with AY-9944 (**30**), although it failed to inhibit aSMase activity in a cell-free system.[71] Tricyclic antidepressants, imipramine (**31**) and desipramine (**32**) (Figure 11), were also reported to decrease aSMase activity in murine neuroblastoma and human fibroblast cell cultures.[72] Interestingly, iminodibenzyl (**33**) (Figure 11) containing the same tricyclic core but devoid of the side chain showed no effect on aSMase activity, indicating the essential role of the cationic amphiphilic characteristics of these molecules. Additional cationic amphiphilic drugs were subsequently found to reduce aSMase activity in cell cultures.[73–76] It is postulated that these molecules accumulate in lysosomes as positively charged species and compete for the aSMase binding site at the inner lysosomal membrane, resulting in a detachment and proteolytic degradation of the enzyme.[76–78] These indirect aSMase inhibitors are now collectively referred to as functional inhibitors of acid sphingomyelinase (FIASMAs).[78] It should be noted that many FIASMAs are FDA approved for clinical use. For instance, the clinical benefit of amitriptyline (**34**) (Figure 11) was investigated in patients with cystic fibrosis, in which ceramide is known to accumulate in bronchial epithelial cells.[79] While FIASMAs offer a unique mechanism to indirectly reduce aSMase activity, their safety profile remains to be seen given that many of these molecules act on various CNS targets.

Screening of tropical plant extracts and microbial secondary metabolites using a crude preparation of aSMase from the bovine brain led to the discovery of some xanthone-based molecules as aSMase inhibitors (Figure 12).[80] α-Mangostin (**35**), cowanol (**36**), and cowanin (**37**) inhibited aSMase with IC_{50} values of 14.1, 10.9, and 19.2 μM, respectively. These inhibitors differ structurally from FIASMAs in that they lack a basic nitrogen atom necessary for amphiphilic properties. Indeed, all of the three compounds inhibited aSMase in a competitive manner with respect to sphingomyelin, suggesting direct interaction with the enzyme. α-Mangostin analog **38** containing saturated side chains retained the inhibitory activity (IC_{50} = 10.9 μM), while diacetyl analog **39** showed no inhibitory activity, highlighting the important role played by the two phenolic OH groups of α-mangostin (**35**) and its derivatives.

Using the γ-pyrone fragment of the xanthone-based inhibitors discussed above as the branching point of origin, a collection of 500 γ-pyrones spanning three hierarchy levels in the branch were assembled for screening.[81] Two potent compounds **40** and **41** containing a benzopyran scaffold (Figure 13) were identified as potent inhibitors of aSMase prepared from rat brain homogenates with IC_{50} values of 3.1 and 9.5 μM, respectively. These compounds displayed no inhibitory activity toward nSMase at concentrations up to 50 μM.

Epicatechin-3-*O*-gallate (**42**) (ECg, Figure 14) was reported to inhibit secretory SMase, a secreted form of aSMase.[82] Further investigation identified a synthetic catechin, 3′-*O*-methylepigallocatechin-3-*O*-gallate (**43**) (EGCg-3′-O-Me, Figure 14), as a low micromolar inhibitor of secretory SMase from rat plasma with an IC_{50} value of 1.7 μM. Secretory SMase was found to be activated by oxidation and inactivated by reduction. Thus, these compounds are believed to act as reducing agents toward the enzyme to achieve its inhibition. Indeed, EGCg-3′-O-Me displayed noncompetitive inhibition when C6 NBD sphingomyelin was

used as a substrate, indicating the presence of an allosteric site targeted by the epicatechin-based compounds.

Weak aSMase inhibitory activity observed for phosphatidylinositol-4,5-bisphosphate (PtdIns4,5P2) against aSMase[83] prompted exploration of other phosphatidylinositol derivatives including PtdIns3,5P2 (**44**) (Figure 15).[84] PtdIns3,5P2 (**44**) potently inhibited a recombinant human aSMase (>90% inhibition at 5 μM) in a micellar assay system. It displayed a noncompetitive mode of inhibition with a K_i value of 0.53 μM and showed no inhibitory activity against rat brain microsomal nSMase at concentrations of up to 50 μM. Subsequently, racemic sulfonate derivatives **45–49** with alkyl groups of varying length (Figure 15) were synthesized in an attempt to remove the polar phosphate moiety of PtdIns3,5P2 (**44**).[85] Compound **49** containing a dodecyl group was found to be most potent against aSMase prepared from rat brain homogenates with an IC_{50} value of 0.90 μM, comparable to that of PtdIns3,5P2 (**44**) (IC_{50} = 0.93 μM). Unlike PtdIns3,5P2 (**44**), however, compound **49** acted as a competitive inhibitor with a K_i value of 0.42 μM, suggesting a mode of binding distinct from that of PtdIns3,5P2 (**44**) despite common structural features shared by the two molecules.

α-Aminobisphosphonate **50** (Figure 16) was identified as a potent aSMase inhibitor (IC_{50} = 0.04 μM) through screening of a bisphosphonate compound library using rat brain homogenates as a source of the enzyme.[86] Additional compounds were synthesized in order to gain further insight into the SAR of bisphosphonate derivatives. Among them, compounds **51–53** (Figure 16) exhibited IC_{50} values below 100 nM. None of these compounds inhibited nSMase of rat brain homogenates.

Cocrystal structure of murine aSMase with compound **51** (PDB code 5FI9) shows that one of the two phosphonate groups in the inhibitor interacts with both zinc atoms in the active site (Figure 17).[66] Compound **51** appears to act as a transition state analog inhibitor by mimicking the intermediate formed by a nucleophilic attack of a water molecule to the phosphodiester of sphingomyelin. Surprisingly, the nine-carbon chain of compound **51** does not seem to bind to the hydrophobic track of aSMase, a putative binding site for the alkyl chains of sphingomyelin.

α-Substituted serinol derivatives **54–57** were reported as aSMase inhibitors in a patent application (Figure 18).[87] The most potent compound **57** containing a 1-nonyl-1*H*-1,2,3-triazol-4-yl group inhibited aSMase with an IC_{50} value of 1.14 μM in a biochemical assay. It is conceivable that the two primary hydroxyl groups of these compounds serve as alternatives to the highly polar phosphonate moieties of **50–53**. Indeed, compound **57** was found to be orally available in mice and distributed to the brain. Furthermore, compound **57** was found to normalize the enhanced brain aSMase activity in APP/PS1 mice to that of wild type.

By use of a pharmacophore model developed from the previously reported xanthone-based aSMase inhibitors, hydroxamate-containing compound **58** (Figure 19) was identified as a submicromolar competitive inhibitor of human aSMase from the supernatants of Huh7 cell lysates with an IC_{50} value of 0.48 μM.[88] Compound **58** was also found to dose-dependently

reduce generation of ceramide and LPS-induced inflammation in human NIH3T3 cells. Subsequent efforts guided by molecular docking led to the discovery of compound **59** devoid of a flexible alkyl chain (Figure 19).[89] Compound **59** inhibited aSMase from the supernatants of Huh7 cell lysates with an IC_{50} value of 0.32 μM. In Sprague-Dawley rats, compound **59** showed good CNS permeability and reduced aSMase activity in cerebral cortex and hippocampus following intraperitoneal injection. Neither **58** nor **59** inhibited nSMase at concentrations up to 100 μM.

4.2. Neutral Sphingomyelinase.

As indicated by its name, the catalytic phosphodiesterase activity of nSMase is optimal at neutral pH. In mammals, four distinct genes, SMPD2–5, have been identified to date, encoding nSMase1–3[90–92] and mitochondria-associated nSMase,[93] respectively. nSMase1–3 show little sequence homology while substantial sequence homology (50.6% similarity) exists between nSMase2 and mitochondria-associated nSMase.[93,94] These isoforms differ in tissue distribution and subcellular localization, suggesting distinct physiological and pathogenic roles.[95]

Similar to aSMase, the therapeutic utility of nSMase inhibition has gained increasing attention as another strategy to regulate ceramide levels in various disease conditions. Most efforts have focused on nSMase2, which is the most extensively studied isoform in terms of its potential as a therapeutic target in a number of disease areas.

nSMase2 contains a hydrophobic N-terminal domain (NTD) and a C-terminal catalytic domain (CAT). The NTD is a lipid-binding domain that interacts with phosphatidylserine (PS), which is required for its full enzymatic activity. The CAT is interrupted by a large insertion (175–339), and the crystal structure of the human nSMase2 CAT devoid of the insertion (residues 117–651 **Δ**175–339) was recently determined at 1.85 Å resolution (PDB code 5UVG).[96] The structure reveals a deoxyribonuclease I (DNase I)-like fold as expected from the structural and catalytic similarity between the two enzymes (Figure 20A). Its active site contains conserved residues within DNase I-like superfamily involved in Mg^{2+} binding and catalysis. The hydrophobic track stretching from the active site is believed to be the binding site for the alkyl chains of sphingomyelin. In this structure, however, an evolutionarily conserved motif termed “DK switch” is positioned such that it obstructs the active site entrance (Figure 20B) and places the conserved Asp430 away from the active site. This observation suggests that “DK switch” adopts different conformations to regulate the enzymatic activity. It was subsequently postulated that PS binding triggers conformational change of “DK switch”, resulting in the formation of the active enzyme.[97] These structural insights should serve as a guide for facilitating the rational design of nSMase inhibitors.

Scyphostatin (**60**), isolated from *Trichopeziza mollissima*, represents the first low-micromolar inhibitor of nSMase.[98] As shown in Figure 21, it bears some structural resemblance to ceramide in that they both contain the *N*-acylamino alcohol scaffold.[99] Scyphostatin (**60**) is a far more potent nSMase inhibitor than other naturally occurring compounds previously reported[100,101] with an IC_{50} value of 1.0 μM using rat brain microsomes as an enzyme source.[102] It showed 50-fold selectivity over aSMase and no inhibitory activity against *Staphylococcus aureus* and *Bacillus cereus* SMases.[102] In

preliminary kinetics studies, scyphostatin (**60**) displayed mixed-type inhibition with respect to sphingomyelin. The presence of the epoxide moiety suggests the possibility of covalent bond formation between the inhibitor and the enzyme though the precise mechanism of inhibition has not yet been elucidated.

Subsequent to the discovery of scyphostatin (**60**), several analogs have been evaluated as nSMase inhibitors (Figure 21). Compound **61** containing a spiroexpoxide moiety exhibited 80% inhibition of nSMase activity in rat brain microsomes following 90 min preincubation at 200 μM.[103,104] It was found that inhibition by compound **61** was time dependent, suggestive of a covalent modification of the enzyme.[103] Compounds **62** and **63** displayed substantially lower inhibitory activity compared to **61**, demonstrating the crucial role played by the primary hydroxyl group in the enzyme inhibition.[104] Because of its structural similarity to scyphostatin (**60**) and compound **61**, manumycin A (**64**) was evaluated for its ability to inhibit nSMase using a partially purified enzyme from rat brain microsomes.[105] Manumycin A (**64**) was, indeed, found to inhibit nSMase in a time-dependent manner (34% inhibition without preincubation and 79% inhibition following 60 min preincubation at 100 μM). Its truncated analog **65** displayed enhanced inhibitory activity (90% inhibition without preincubation and 98% inhibition following 60 min preincubation at 100 μM), while analog **66** (racemic) containing a saturated acyl group showed weaker activity (10% inhibition without preincubation and 88% inhibition following 60 min preincubation at 100 μM). Although these analogs were not directly (head-to-head) compared to scyphostatin, it appears that none of them exceeded the inhibitory potency achieved by scyphostatin (**60**).

Alutenusin (**67**) (Figure 22), originally isolated from *Alternaria* sp., was identified as an nSMase inhibitor through microbial screening.[106] Alutenusin (**67**) containing a biphenyl scaffold is one of the first nSMase inhibitors structurally distinct from sphingolipids and was found to inhibit nSMase from rat brain microsomes with a K_i value of 20 μM. As expected from its non-sphingolipid-like structure, alutenusin (**67**) displayed a noncompetitive inhibition with respect to sphingomyelin. Furthermore, it showed no inhibitory activity against aSMase from rat brain microsomes at concentrations up to 950 μM.

Hydroquinones **68–70** (Figure 23), isolated from *Acre-monium murorum*, were reported to inhibit nSMase of rat brain microsomes with IC_{50} values of 7.2 μg/mL (34 μM), 3.6 μg/mL (17 μM), and 3.2 μg/mL (16 μM), respectively.[107] Compound **71** (Figure 23), the corresponding quinolone derivative of **69**, was also found to potently inhibit nSMase of rat brain microsomes with a IC_{50} value of 0.8 μg/mL (4.2 μM).[108] Another hydroquinone-based compound, ubiquinol (**72**) ($CoQ_{10}H_2$, Figure 23), was reported to inhibit Mg^{2+}-dependent nSMase of pig liver plasma membranes (>90% inhibition at 100 μM following 15 min preincubation) in a noncompetitive manner with respect to sphingomyelin.[109] Subsequent studies releveled that inhibition by ubiquinol (**72**) is time-dependent, displaying a greater degree of potency when preincubated for 60 min.[110] Furthermore, CoQ_6H_2 (**73**) (Figure 23) was found to have the optimal isoprenoid side chain length for nSMase inhibition among several homologs.[110]

In an attempt to mimic the phosphodiester moiety of sphingomyelin, some phosphorus-based compounds have also been examined as nSMase inhibitors. After some early efforts

resulting in identification of weak nSMase inhibitors,[111,112] compound **74** (Figure 24) was found to inhibit nSMase of bovine brain microsomes with an IC_{50} value of 3.3 μM.[113] It should be noted that the stereochemistry of **74** is opposite that of sphingomyelin at both of the two chiral centers. Surprisingly, compound **75** possessing the same stereochemistry as sphingomyelin (Figure 24) showed much weaker inhibitory potency (IC_{50} = 181 μM). These findings indicate that compound **74** does not act as a substrate-based inhibitor despite its structural similarity to sphingomyelin. Indeed, compound **74** displayed noncompetitive inhibition with respect to sphingomyelin with a K_i value of 1.6 μM. Consistent with its mode of inhibition, compound **74** showed no inhibitory effect on SMase from *B. cereus* even though it shares common structural and mechanistic features in the catalytic domain with mammalian nSMase.

Some sphingomyelin analogs possessing a carbamate moiety as a replacement for the phosphodiester group were identified as low-micromolar nSMase inhibitors (Figure 25).[114] By use of rat brain microsomes as the enzyme source, carbamates **76** and **77** were found to inhibit nSMase with IC_{50} values of 2.8 and 1.8 μM, respectively. SAR studies indicate that only a narrow range of acyl groups are tolerated at the amino group. Both *N*-acetyl and *N*-stearoyl derivatives **78** and **79** showed no inhibitory activity at concentrations up to 100 μM.

Ceramide derivatives **80** and **81** containing a thiourea moiety (Figure 26) were reported to inhibit nSMase semipurified from bovine brain microsomes with low micromolar potency in a time-dependent manner (~90% inhibition after **60** min preincubation).[115] Compounds **80** and **81** displayed competitive inhibition with respect to sphingomyelin with K_i values of 1.7 and 2.5 μM, respectively, suggesting direct binding of these ceramide derivatives to the active site of the enzyme. Assuming that the primary hydroxyl group of these inhibitors corresponds to that of ceramide, the stereochemistry of the amino-attached (*R*)-chiral carbon appears opposite to that of ceramide. The corresponding (*S*)-derivatives of 80 and 81, however, were not explored in this report.

Ceramide derivatives containing a lactone moiety in their sphingosine component were found to inhibit nSMase from rat brain microsomes (Figure 27).[116] Compounds **82** and **83**, the so-called sphingolactones, achieved nearly 50% and 90% inhibition following 15 min of preincubation at 350 μM. It is speculated that the time-dependent inhibition resulted from irreversible covalent binding of the lactone carbonyl moiety to the enzyme.

Aminoguanidine derivatives C11AG (**84**) and **85** (Figure 28) were reported to inhibit nSMase activity of rat brain microsomes with IC_{50} values of 8.2 and 5 μM, respectively.[117] Although C11AG (**84**) is less potent than compound **85**, it displayed superior antiviral potency against HSV-1 in Rita cells with a favorable therapeutic index. C11AG (**84**) showed 30-fold selectivity over aSMase and no inhibitory activity toward other phospholipases including phospholipase A2, phospholipase D, and phosphatidylcholine-specific phospholipase C. In subsequent studies, C11AG (**84**) was found to suppress LPS-stimulated sphingomyelin degradation and ceramide synthesis in RAW cells, resulting in suppression of NF-κB liberation.[118] Another aminoguanidine derivative, ES048 (**86**) (Figure 28), was reported to inhibit nSMase activity in mouse splenocytes though it exhibited a U-shaped

dose–response curve with the maximal effect (~80% inhibition) at 1 μM.[119] It showed no inhibitory effects on either aSMase from mouse splenocytes or recombinant human aSMase.

Some N-dialkylated amino acids were reported as low micromolar nSMase inhibitors (Figure 29).[120] Among the compounds tested, serine and alanine derivatives **87** and **88** were most potent with IC_{50} values of 1.8 and 2.8 μM, respectively, using U937 cell lysate as a source of the enzyme. Preliminary SAR studies indicated that the carboxyl group and the propenyl (−C=CH–CH_2−) linkers are essential for the potent inhibitory activity.

GW4869 (**89**) (Figure 30) was identified by a high throughput assay using a partially purified and delipidated rat brain nSMase.[121] GW4869 (**89**) is a noncompetitive inhibitor with respect to sphingomyelin with an IC_{50} value of 1 μM. GW4869 (**89**) showed no inhibitory activity against human aSMase. Interestingly, PS, a known endogenous activator of nSMase,[122] was found to reduce the inhibitory potency of GW4869 (**89**). The two substances, however, were unlikely to compete for the same binding site since a PS-independent *B. cereus* SMase was also inhibited by GW4869 (**89**) with similar potency. GW4869 (**89**) significantly inhibited TNF-induced sphingomyelin hydrolysis in a dose-dependent manner in MCF7 cells, while it showed no effects on the de novo ceramide biosynthetic pathway.[122] Since its discovery, GW4869 (**89**) has been by far the most widely used prototype nSMase2 inhibitor for studying the physiological and pathological roles of nSMase. Indeed, as an *in vivo* probe molecule, GW4869 (**89**) has demonstrated the therapeutic utility of nSMase2 inhibition in a variety of animal disease models, including Alzheimer's disease,[123,124] traumatic brain injury,[125] lung injury,[126] metabolic disease,[127] heart failure,[128] and cancer.[129,130] Despite its proven track record as a tool compound, systematic structural optimization efforts on GW4869 (**89**) has not yet been reported, presumably due to its high lipophilic core scaffold contributing to poor aqueous solubility.

Various 4*H*-1,2,4-triazole-3(2*H*)-thione derivatives were reported as low micromolar nSMase inhibitors (Figure 31). Compounds **90** and **91** inhibited mouse nSMase with IC_{50} values of 2.5 and 2.4 μM, respectively.[131] The same group also reported a series of 3,4-dihydropyrimidine-2(1*H*)-thione derivatives including **92** and **93** (Figure 31) as nSMase inhibitors with IC_{50} values of 0.9 and 0.86 μM, respectively. More recently, cambinol (**94**) (Figure 31), a 2-thioxo-2,3-dihydropyrimidin-4(1*H*)-one derivative originally reported as a SIRT1/2 inhibitor,[132] was identified as a nSMase2 inhibitor from screening assays using the recombinant human enzyme.[133] Cambinol (**94**) displayed uncompetitive inhibition with respect to sphingomyelin with a K_i value of 7 μM. It also inhibited nSMase activity of *B. cereus* and rat brain homogenate with IC_{50} values of 5 and 6 μM, respectively. Furthermore, cambinol was found to block TNF-α induced increase in ceramide levels in the rat primary neurons. It should be noted that inhibitors **90–94** possess the cyclic thiourea moiety as the common structural feature. In particular, it is conceivable that the pyrimidine-based core rings of compounds **92–94** play a similar role in binding to the enzyme. Cambinol (**94**) was independently identified as a tau propagation inhibitor from cell-based functional assays.[134] Molecular docking and molecular dynamic simulation studies using recently published crystal structure of nSMase2 CAT[96] indicate that it binds to nSMase2 at the DK switch and inhibits the enzyme by directing Asp430 away from the active site.[134]

2,6-Dimethoxy-4-(5-phenyl-4-thiophen-2-yl-1*H*-imidazol-2-yl)phenol (**95**) (DPTIP, Figure 32) was identified as a potent inhibitor of human nSMase2 through a high throughput screening of >365 000 compounds from the Molecular Libraries Small Molecule Repository (MLSMR) and the NCGC Pharmaceutical Collection (NPC).[135] DPTIP (**95**) inhibited a human recombinant nSMase2 with an IC_{50} value of 30 nM in a noncompetitive manner with respect to sphingomyelin. DPTIP (**95**) inhibited release of extracellular vesicles from the rat primary astrocyte cultures in a dose dependent manner. Furthermore, DPTIP (**95**) attenuated IL-1β-induced astrocyte-derived extracellular vesicle (ADEV) release in GFAP-GFP mice following intraperitoneal administration. Subsequent medicinal chemistry efforts identified 4-(1*H*-imidazol-2-yl)-2,6-dimethoxyphenol as a key pharmacophore essential for the potent nSMase2 inhibition, and several derivatives containing this pharmacophore exhibited inhibitory potency comparable to that of DPTIP, including compounds **96–99** (Figure 32).[136]

Compound 100 containing an imidazo[1,2-*b*]pyridazine ring is another inhibitor identified from screening efforts using a human recombinant nSMase2.[137,138] Preliminary SAR studies revealed that the imidazo[1,2-*b*]pyridazin-8-amine scaffold is essential for the potent inhibition as compounds possessing other 6,5-fused ring scaffolds failed to show any inhibitory activity. On the other hand, modifications of the pyrrolidine ring of **100** led to the discovery of phenyl (*R*)-(1-(3-(3,4-dimethoxyphenyl)-2,6-dimethylimidazo[1,2-*b*]pyridazin-8-yl)-pyrrolidin-3-yl)carbamate (**101**) (PDDC) with improved potency (IC_{50} = 0.3 μM).[137] It displayed a noncompetitive inhibition with respect to sphingomyelin with a K_i value of 0.3 μM. Consistent with its noncompetitive mode of inhibition, PDDC (**101**) showed no inhibitory activity against aSMase and two other phosphodiesterases (PDE3A and PDE4D2). It was found to be metabolically stable and orally available in mice with excellent CNS permeability. As seen with DPTIP, but by oral administration, PDDC (**101**) inhibited ADEV release in a dose dependent manner in GFAP-GFP mice.[137] It was also reported to reverse cognitive impairment in 5XFAD mice following intraperitoneal administration.[138] Subsequently, extensive structure–activity relationship (SAR) studies were conducted using PDDC as a molecular template, providing additional potent nSMase2 inhibitors (Figure 33) within this structural series including compounds **102** (IC_{50} = 0.1 μM) and **103** (IC_{50} = 0.07 μM).[138]

Targeting both nSMase2 and acetylcholinesterase (AChE) may lead to a new therapeutic approach to Alzheimer's disease since it could not only suppress exosome biogenesis but also enhance cholinergic synaptic plasticity. To this end, a ~70-compound library largely comprising phenserine analogs and other known AChE inhibitors was screened for nSMase2 inhibitory activity.[139] One hit from the screening, compound **104** (Figure 34), was validated as a weak inhibitor of nSMase2 (60% inhibition at 50 μM). Subsequent hit-to-lead optimization led to the discovery of compounds **105** and **106** (Figure 34) displaying nearly 100-fold more potent inhibitory activity. As anticipated from their phensvenine-like structures,[140] compounds **105** and **106** were also found to inhibit AChE with IC_{50} values of 7 and 1.7 μM, respectively. Both compounds displayed an uncompetitive mechanism of inhibition with respect to sphingomyelin. Consistent with these findings, molecular docking analysis using a crystal structure of the nSMase2 CAT (PDB code 5UVG) indicates that both compounds bind to nSMase2 at the DK-switch and stabilize its inactive conformation[139] in a

manner similar to what was proposed for cambinol (**94**).[134] Both compounds were reported to suppress the release of tau-bearing extracellular vesicles (EVs) in cell-based assays, and compound **106** significantly reduced IL1β-induced release of tau-carrying exosomes in tau P301S (PS19 line) mice.[139]

4.3. Bacterial Sphingomyelinase.

There are two different types of bacterial SMase depending on the phosphodiester cleaving site.[16] Like human SMase, sphingomyelinase C (SMaseC) catalyzes the hydrolysis of the phosphoester linkage between ceramide and phosphocholine. Sphingomyelinase D, on the other hand, hydrolyzes the other phosphoester bond, resulting in the release of ceramide-1-phosohate and choline. Given the primary focus of this review article on ceramide-producing enzymes, only SMaseC inhibitors will be discussed herein. SMaseC can be found in many species of bacteria, including *S. aureus*, *B. cereus*, *Clostridium perfringens*, and *Leptospira interrogans*.[16] It appears that SMaseC is evolutionally related to mammalian neutral sphingomyelinases as they share a number of conserved residues in the catalytic region and adopt the same fold as DNase I, another metal-dependent phosphodiesterase. Indeed, mammalian nSMase1 and nSMase2 were cloned based on their sequence homology to bacterial SMaseC.[90,91] SMaseC, however, differs from the mammalian homologs in that it is a secretory protein that can target the host cell plasma membrane. For instance, increase in ceramide caused by SMaseC is known to alter the physical properties of the host cell plasma membrane and, possibly, contribute to the pathogenesis of some infectious diseases.[16] In fact, antibodies against SMaseC, but not those against phosphatidylcholine and phosphatidylinositol-specific phospholipases C, were found to protect mice from a lethal dose of *B. cereus*,[141] underscoring the potential therapeutic utility of SMaseC inhibitors.

Prior to the elucidation of human nSMase2 crystal structure,[96] a number of crystal structures have been solved for SMaseC.[142–145] The first crystal structure of SMaseC was determined for *Listeria ivanovii* SMaseC (SmcL) at 1.9 Å resolution (PDB code 1ZWX).[142] Like human nSMase2, SmcL adopts a DNase I-like protein fold and possesses a number of key residues in the active site conserved among bacterial SMases and eukaryotic nSMases (Figure 35A), suggesting a common catalytic mechanism for binding and hydrolysis of sphingomyelin. The structure also revealed a large hydrophobic β-hairpin and hydrophobic loop surrounding the active site. In the absence of identifiable membrane-spanning regions, these segments unique to bacterial SMases are thought to play an important role in mediating protein–host membrane interactions to guide the phosphodiester moiety of sphingomyelin into the active site (Figure 35B). It should be noted that, unlike the human nSMase2 CAT structure (PDB code 5UVG) discussed earlier, the DK switch in this structure forms a short α-helix that directs the conserved Asp160 residue into the active site, conceivably representing the active conformation of the enzyme.

As could be expected from the close evolutionary relationship between the two classes of enzymes, some mammalian nSMase inhibitors, including GW4869 (**89**) and cambinol (**94**), were also found to inhibit *B. cereus* SMaseC as described earlier.[122,133] Conversely, it is conceivable that some of the SMaseC inhibitors described below act as mammalian nSMase inhibitors.

Phosphonate-based sphingomyelin analogs **107** and **108** (Figure 36) were explored as transition-state analog inhibitors of sphingomyelinase.[146,147] Compounds **107** and **108**, however, showed rather weak inhibitory potency against *B. cereus* SMaseC with IC_{50} values of 120 μM and 78 μM, respectively.[147] Phosphoramidate **109**[148] and difluoromethylene phosphonate **110**[149] (Figure 36) also exhibited low inhibitory potency against *B. cereus* SMaseC with IC_{50} values of **53** and **57** μM, respectively. The weak inhibitory activity of these compounds can be at least partially attributed to the lack of the double bond corresponding to the C4–C5 double bond of sphingomyelin. Despite the presence of the C4–C5 double bond, however, the inhibitory activity of thiophosphate derivative **111** (Figure 36) was reported to be even weaker than other phosphorus-based compounds.[150] It was found, however, that compound **111** can be recognized as a substrate by *B. cereus* SMaseC, releasing 1-thiosphingosine. Since the free thiol group can be captured by various labeling reagents as generated, compound **111** may serve as a useful substrate to continuously monitor SMaseC activity.

On the basis of the inspection of the *B. cereus* SMaseC crystal structures,[143] sphingomyelin analog **112** containing a bipyridyl moiety (Figure 37) was designed to interact with the active site Mg^{2+} ion, predicted to play a critical role in the catalytic process.[151] Compound **112** inhibited *B. cereus* SMaseC with an IC_{50} value of 1.2 μM. It displayed a competitive inhibition with respect to sphingomyelin with a K_i value of 5.2 μM, indicating that the inhibitor competes with the substrate at the active site of the enzyme as designed. Compound **113** (Figure 37), a regioisomer of **112** with a bipyridyl moiety linked to the C3 secondary hydroxyl group, showed only weak inhibitory activity (20% inhibition at 100 μM). Docking simulation analyses suggest that the bipyridyl moiety of compound **112** is optimally positioned to participate in the coordination with the active site Mg^{2+} ion while that of compound **113** is oriented away from the active site.[151] Subsequent structural optimization efforts led to the discovery of two submicromolar inhibitors **114** and **115** (Figure 37).[152] Compound **114**, devoid of an acyl group, inhibited *B. cereus* SMaseC with an IC_{50} value of 0.9 μM. Compound **115** has a phenyl group replacing the alkenyl chain extending from the C3 position and inhibited *B. cereus* SMaseC with an IC_{50} value of 0.8 μM. Like compound **112**, the two inhibitors displayed a competitive inhibition with respect to sphingomyelin with K_i values of 2.8 and 1.3 μM, respectively. Intraperitoneal injection of compound **115** in mice decreased the lethality of the *B. cereus* treatment in a dose-dependent manner, demonstrating for the first time *in vivo* efficacy of a small molecule SMaseC inhibitor.[152]

5. OTHER CERAMIDE-PRODUCING ENZYMES

In addition to the enzymes involved in the three major ceramide biosynthesis pathways described above, glucocerebrosidase, galactocerebrosidase, and ceramide-1-phosphate phosphatase are known to produce ceramide from distinct substrates (Figure 1). Ceramide-1-phoshate can be hydrolyzed by phosphatidate phosphohydrolase,[153] presumably owing to its overall structural similarity to phosphatidate. Although definitive evidence for the existence of monophosphatase specific to ceramide-1-phosphate remains to be seen, it has been implicated that ceramide-1-phosphate phosphatase activities detected in brain

synaptosomes[154] and liver plasma membrane fractions[155] are distinct from that of phosphatidate phosphatase. Such enzyme, if identified, could serve as another therapeutic target aimed at regulating ceramide biosynthesis. Glucocerebrosidase and galactocerebrosidase are lysosomal glycoside hydrolases that cleave glucosylceramide and galactosylceramide, respectively, resulting in the generation of ceramide (Figure 1). The physiological and pathological significance of ceramide produced by these enzymes has not yet been extensively studied. However, accumulation of glucosylceramide due to inherited deficiency of glucocerebrosidase is linked to a rare genetic lysosomal storage disorder, Gaucher disease.[156] On the other hand, Krabbe disease, another genetic lysosomal storage disorder, is known to be caused by a deficiency in galactocerebrosidase, which leads to the accumulation of galactosylceramide.[157] Mutations in these enzymes commonly result in protein misfolding and subsequent premature degradation in the ER. To this end, interests in developing inhibitors of these enzymes have been predominantly driven by the goal of identifying molecular chaperones capable of stabilizing the native conformation of the mutant enzymes and increasing translocation of functional enzymes to the lysosomes. For instance, ambroxol (**116**) (Figure 38) was reported to act as a mixed-type inhibitor of human recombinant glucocerebrosidase at the neutral pH found in the ER and to display no inhibitory activity at the acidic pH of lysosomes.[158] This pH dependent inhibitory action makes ambroxol (**116**) an ideal pharmacological chaperone for mutant glucocerebrosidases. Indeed, treatment with ambroxol (**116**) resulted in the increase of glucocerebrosidase activity and protein levels in N370S/N370S GD-1 fibroblast cell line.[158] It should be noted that there have been active research efforts to develop pharmacological chaperones for lysosomal enzymes as new therapeutic options for various types of genetic lysosomal storage disorders including Gaucher and Krabbe diseases. Excellent review articles focused on the medicinal chemistry aspects of these efforts have been published in recent years.[159,160]

6. CONCLUSION

The intricate metabolic network surrounding ceramide reflects the dynamic role played by ceramide at the core of sphingolipid metabolism pathways in both physiological and pathological conditions. The fact that several distinct enzymes can each produce ceramide has provided potentially important therapeutic opportunities by inhibiting specific ceramide-producing enzymes depending on the disease of interest. As described in this review article, tremendous efforts have been devoted to identifying small molecule inhibitors of these enzymes. Upon review of the structural evolution of these inhibitors, one notable trend appears to be a departure from lipid-like scaffolds originating from the structures of substrates. This movement has been most likely driven by a strong desire to identify more drug-like inhibitors that can serve not only as biological probe molecules but also as lead molecules for future therapeutic development. In particular, DES1 inhibitor SKI II (**8**), CerS1 inhibitor P053 (**29**),[60] aSMase inhibitor **59**,[89] and nSMase2 inhibitors DPTIP (**95**),[135] PDDC (**101**),[137] and **106**[139] represent promising leads for further optimization as these compounds displayed not only submicromolar inhibitory potency but also desirable *in vivo* pharmacokinetics and promising *in vivo* profile as summarized in Table 1.

Despite the growing interest in ceramide-producing enzymes as therapeutic targets, exploration of structure-based drug design has been limited to aSMase[89] and *B. cereus*

SMaseC.[151] Further progress in structural biology is crucial for successful development of structure-based drug design strategies for inhibitors of other ceramide-producing enzymes. While the recent elucidation of the crystal structure of human nSMase2 catalytic domain[96] is an important breakthrough, the full-length structure of nSMase2 would be highly desirable given that many nSMase inhibitors do not appear to bind to the active site.

Finally, recent advancement in the field of sphingolipidomics[161,162] is highly encouraging and relevant to inhibitors of ceramide-producing enzymes given that the use of reliable biomarkers is becoming increasingly important in successful translation of experimental drugs into clinical development.[163] Application of the most advanced sphingolipidomics analysis techniques in clinical studies should provide in-depth information on the metabolic consequence(s) of inhibiting specific ceramide producing enzymes, enabling informed decision making at various stages of clinical development. It is certainly a very exciting time to explore therapeutics for many disease areas by targeting ceramide biosynthesis.

ACKNOWLEDGMENTS

The authors of this manuscript have been supported by NIH Grants P30MH075673 (B.S.S) and R01AG059799 (B.S.S. and T.T.) and a Tau Pipeline Enabling Program Grant T-PEP-18–579974C jointly funded by the Alzheimer's Association and Rainwater Charitable Foundation (to B.S.S). The authors are also grateful for the support provided by the Bloomberg-Kimmel Institute for Cancer Immunotherapy at Johns Hopkins.

Biographies

Jan Skácel received his Ph.D. in Medicinal Chemistry from the University of Chemistry and Technology, Prague. As a Ph.D. student, he worked at the Institute of Organic Chemistry and Biochemistry of the Czech Academy of Sciences under the direction of Dr. Zlatko Janeba. His doctoral research was mainly focused on the design and synthesis of novel PNP and HG(X)PRT inhibitors. Currently, Dr. Skácel is a postdoctoral fellow at Johns Hopkins University, where he explores the design and synthesis of novel nSMase2 inhibitors under the direction of Prof. Takashi Tsukamoto.

Barbara S. Slusher is Professor of Neurology, Pharmacology, Neuroscience, Psychiatry, Medicine, and Oncology and the Director of Johns Hopkins Drug Discovery at Johns Hopkins School of Medicine. Prior to joining Johns Hopkins in September 2009, she spent 18 years in the pharmaceutical industry. She has extensive experience in drug discovery spanning through phase I/IIa clinical development. She is an inventor of over 80 issued patents and applications and an author of over 250 scientific articles. She serves on the board or as a scientific consultant to multiple biotechnology companies and cofounded the first International Academic Drug Discovery Consortium.

Takashi Tsukamoto is Associate Professor of Neurology at Johns Hopkins University and the Director of Medicinal Chemistry at Johns Hopkins Drug Discovery. He received his Ph.D. in Chemistry from Tokyo Institute of Technology and pursued his postdoctoral studies at the University of Michigan. Prior to joining Johns Hopkins in 2009, Dr. Tsukamoto has held a variety of research positions in the pharmaceutical industry. During the course of his career, he has served as a lead medicinal chemist in a number of drug discovery projects, exploring new therapeutics for neurological disorders and cancer. He is the lead inventor of

the cytidine deaminase inhibitor cedazuridine and its combination with decitabine, which received FDA approval as Inqovi in 2020.

ABBREVIATIONS USED

AChE	acetylcholinesterase
CerS	ceramide synthase
DES1	dihydroceramide desaturase 1
FIASMAs	functional inhibitors of acid sphingomyelinase
PDB	Protein Data Bank
PS	phosphatidylserine
SMase	sphingomyelinase

REFERENCES

(1). Fahy E; Subramaniam S; Brown HA; Glass CK; Merrill AH Jr.; Murphy RC; Raetz CR; Russell DW; Seyama Y; Shaw W; Shimizu T; Spener F; van Meer G; VanNieuwenhze MS; White SH; Witztum JL; Dennis EA A comprehensive classification system for lipids. J. Lipid Res 2005, 46, 839–861. [PubMed: 15722563]

(2). Wattenberg BW The long and the short of ceramides. J. Biol. Chem 2018, 293, 9922–9923. [PubMed: 29934368]

(3). Gault CR; Obeid LM; Hannun YA An overview of sphingolipid metabolism: From synthesis to breakdown. Adv. Exp. Med. Biol 2010, 688, 1–23. [PubMed: 20919643]

(4). Stiban J; Tidhar R; Futerman AH Ceramide synthases: Roles in cell physiology and signaling. Adv. Exp. Med. Biol 2010, 688, 60–71. [PubMed: 20919646]

(5). Reynolds CP; Maurer BJ; Kolesnick RN Ceramide synthesis and metabolism as a target for cancer therapy. Cancer Lett 2004, 206, 169–180. [PubMed: 15013522]

(6). Hannun YA; Obeid LM Sphingolipids and their metabolism in physiology and disease. Nat. Rev. Mol. Cell Biol 2018, 19, 175–191. [PubMed: 29165427]

(7). Rodriguez-Cuenca S; Barbarroja N; Vidal-Puig A Dihydroceramide desaturase 1, the gatekeeper of ceramide induced lipotoxicity. Biochim. Biophys. Acta, Mol. Cell Biol. Lipids 2015, 1851, 40–50.

(8). Fabrias G; Munoz-Olaya J; Cingolani F; Signorelli P; Casas J; Gagliostro V; Ghidoni R Dihydroceramide desaturase and dihydrosphingolipids: Debutant players in the sphingolipid arena. Prog. Lipid Res 2012, 51, 82–94. [PubMed: 22200621]

(9). Park JW; Park WJ; Futerman AH Ceramide synthases as potential targets for therapeutic intervention in human diseases. Biochim. Biophys. Acta, Mol. Cell Biol. Lipids 2014, 1841, 671–681.

(10). Cingolani F; Futerman AH; Casas J Ceramide synthases in biomedical research. Chem. Phys. Lipids 2016, 197, 25–32. [PubMed: 26248326]

(11). Gulbins E; Walter S; Becker KA; Halmer R; Liu Y; Reichel M; Edwards MJ; Muller CP; Fassbender K; Kornhuber J A central role for the acid sphingomyelinase/ceramide system in neurogenesis and major depression. J. Neurochem 2015, 134, 183–192. [PubMed: 25925550]

(12). Park MH; Jin HK; Bae JS Potential therapeutic target for aging and age-related neurodegenerative diseases: The role of acid sphingomyelinase. Exp. Mol. Med 2020, 52, 380–389. [PubMed: 32203096]

(13). Kornhuber J; Rhein C; Muller CP; Muhle C Secretory sphingomyelinase in health and disease. Biol. Chem 2015, 396, 707–736. [PubMed: 25803076]

(14). Clarke CJ; Wu BX; Hannun YA The neutral sphingomyelinase family: Identifying biochemical connections. Adv. Enzyme Regul 2011, 51, 51–58. [PubMed: 21035485]

(15). Shamseddine AA; Airola MV; Hannun YA Roles and regulation of neutral sphingomyelinase-2 in cellular and pathological processes. Adv. Biol. Regul 2015, 57, 24–41. [PubMed: 25465297]

(16). Flores-Diaz M; Monturiol-Gross L; Naylor C; Alape-Giron A; Flieger A Bacterial sphingomyelinases and phospholipases as virulence factors. Microbiol. Mol. Biol. Rev 2016, 80, 597–628. [PubMed: 27307578]

(17). Delgado A; Casas J; Llebaria A; Abad JL; Fabrias G Inhibitors of sphingolipid metabolism enzymes. Biochim. Biophys. Acta, Biomembr 2006, 1758, 1957–1977.

(18). Arenz C Small molecule inhibitors of acid sphingomyelinase. Cell. Physiol. Biochem 2010, 26, 1–8. [PubMed: 20501999]

(19). Bhabak KP; Arenz C Novel drugs targeting sphingolipid metabolism. Handb. Exp. Pharmacol 2013, 215, 187–196.

(20). Adada M; Luberto C; Canals D Inhibitors of the sphingomyelin cycle: Sphingomyelin synthases and sphingomyelinases. Chem. Phys. Lipids 2016, 197, 45–59. [PubMed: 26200918]

(21). Casasampere M; Ordonez YF; Pou A; Casas J Inhibitors of dihydroceramide desaturase 1: Therapeutic agents and pharmacological tools to decipher the role of dihydroceramides in cell biology. Chem. Phys. Lipids 2016, 197, 33–44. [PubMed: 26248324]

(22). Karsai G; Kraft F; Haag N; Korenke GC; Hanisch B; Othman A; Suriyanarayanan S; Steiner R; Knopp C; Mull M; Bergmann M; Schroder JM; Weis J; Elbracht M; Begemann M; Hornemann T; Kurth I Degs1-associated aberrant sphingolipid metabolism impairs nervous system function in humans. J. Clin. Invest 2019, 129, 1229–1239. [PubMed: 30620338]

(23). Breen P; Joseph N; Thompson K; Kraveka JM; Gudz TI; Li L; Rahmaniyan M; Bielawski J; Pierce JS; van Buren W; Bhatti G; Separovic D Dihydroceramide desaturase knockdown impacts sphingolipids and apoptosis after photodamage in human head and neck squamous carcinoma cells. Anticancer Res 2013, 33, 77–84. [PubMed: 23267130]

(24). Ordonez-Gutierrez L; Benito-Cuesta I; Abad JL; Casas J; Fabrias G; Wandosell F Dihydroceramide desaturase 1 inhibitors reduce amyloid-beta levels in primary neurons from an Alzheimer's disease transgenic model. Pharm. Res 2018, 35, 49. [PubMed: 29411122]

(25). Chaurasia B; Tippetts TS; Mayoral Monibas R; Liu J; Li Y; Wang L; Wilkerson JL; Sweeney CR; Pereira RF; Sumida DH; Maschek JA; Cox JE; Kaddai V; Lancaster GI; Siddique MM; Poss A; Pearson M; Satapati S; Zhou H; McLaren DG; Previs SF; Chen Y; Qian Y; Petrov A; Wu M; Shen X; Yao J; Nunes CN; Howard AD; Wang L; Erion MD; Rutter J; Holland WL; Kelley DE; Summers SA Targeting a ceramide double bond improves insulin resistance and hepatic steatosis. Science 2019, 365, 386–392. [PubMed: 31273070]

(26). Triola G; Fabrias G; Llebaria A Synthesis of a cyclopropane analogue of ceramide, a potent inhibitor of dihydroceramide desaturase. Angew. Chem., Int. Ed 2001, 40, 1960–1962.

(27). Johnson AR; Pearson JA; Shenstone FS; Fogerty AC Inhibition of the desaturation of stearic to oleic acid by cyclopropene fatty acids. Nature 1967, 214, 1244–1245. [PubMed: 6066117]

(28). Triola G; Fabrias G; Casas J; Llebaria A Synthesis of cyclopropene analogues of ceramide and their effect on dihydroceramide desaturase. J. Org. Chem 2003, 68, 9924–9932. [PubMed: 14682684]

(29). Triola G; Fabrias G; Dragusin M; Niederhausen L; Broere R; Llebaria A; van Echten-Deckert G Specificity of the dihydroceramide desaturase inhibitor n-[(1r,2s)-2-hydroxy-1-hydroxymethyl-2-(2-tridecyl-1-cyclopropenyl)ethyl]octanami de (gt11) in primary cultured cerebellar neurons. Mol. Pharmacol 2004, 66, 1671–1678. [PubMed: 15371559]

(30). Pou A; Abad JL; Ordonez YF; Garrido M; Casas J; Fabrias G; Delgado A From the configurational preference of dihydroceramide desaturase-1 towards delta(6)-unsaturated substrates to the discovery of a new inhibitor. Chem. Commun 2017, 53, 4394–4397.

(31). Munoz-Olaya JM; Matabosch X; Bedia C; Egido-Gabas M; Casas J; Llebaria A; Delgado A; Fabrias G Synthesis and biological activity of a novel inhibitor of dihydroceramide desaturase. ChemMedChem 2008, 3, 946–953. [PubMed: 18236489]

(32). Buist PH; Dallmann HG; Rymerson RR; Seigel PM; Skala P Use of sulfur as an oxidant detector. Tetrahedron Lett 1988, 29, 435–438.

(33). Hovik KE; Spydevold OS; Bremer J Thia fatty acids as substrates and inhibitors of stearoyl-coa desaturase. Biochim. Biophys. Acta, Lipids Lipid Metab 1997, 1349, 251–256.

(34). Bedia C; Triola G; Casas J; Llebaria A; Fabrias G Analogs of the dihydroceramide desaturase inhibitor gt11 modified at the amide function: Synthesis and biological activities. Org. Biomol. Chem 2005, 3, 3707–3712. [PubMed: 16211106]

(35). Camacho L; Simbari F; Garrido M; Abad JL; Casas J; Delgado A; Fabrias G 3-deoxy-3,4-dehydro analogs of xm462. Preparation and activity on sphingolipid metabolism and cell fate. Bioorg. Med. Chem 2012, 20, 3173–3179. [PubMed: 22537678]

(36). Moon RC; Thompson HJ; Becci PJ; Grubbs CJ; Gander RJ; Newton DL; Smith JM; Phillips SL; Henderson WR; Mullen LT; Brown CC; Sporn MB N-(4-hydroxyphenyl)-retinamide, a new retinoid for prevention of breast cancer in the rat. Cancer Res 1979, 39, 1339–1346. [PubMed: 421218]

(37). Kraveka JM; Li L; Szulc ZM; Bielawski J; Ogretmen B; Hannun YA; Obeid LM; Bielawska A Involvement of dihydroceramide desaturase in cell cycle progression in human neuroblastoma cells. J. Biol. Chem 2007, 282, 16718–16728. [PubMed: 17283068]

(38). Rahmaniyan M; Curley RW Jr.; Obeid LM; Hannun YA; Kraveka JM Identification of dihydroceramide desaturase as a direct in vitro target for fenretinide. J. Biol. Chem 2011, 286, 24754–24764. [PubMed: 21543327]

(39). French KJ; Upson JJ; Keller SN; Zhuang Y; Yun JK; Smith CD Antitumor activity of sphingosine kinase inhibitors. J. Pharmacol. Exp. Ther 2006, 318, 596–603. [PubMed: 16632640]

(40). Gao P; Peterson YK; Smith RA; Smith CD Characterization of isoenzyme-selective inhibitors of human sphingosine kinases. PLoS One 2012, 7, No. e44543.

(41). Cingolani F; Casasampere M; Sanllehi P; Casas J; Bujons J; Fabrias G Inhibition of dihydroceramide desaturase activity by the sphingosine kinase inhibitor ski ii. J. Lipid Res 2014, 55, 1711–1720. [PubMed: 24875537]

(42). Aurelio L; Scullino CV; Pitman MR; Sexton A; Oliver V; Davies L; Rebello RJ; Furic L; Creek DJ; Pitson SM; Flynn BL From sphingosine kinase to dihydroceramide desaturase: A structure-activity relationship (sar) study of the enzyme inhibitory and anticancer activity of 4-((4-(4-chlorophenyl)thiazol-2-yl)amino)-phenol (ski-ii). J. Med. Chem 2016, 59, 965–984. [PubMed: 26780304]

(43). Romero DL; Mccall JM; Blitzer J Inhibitors of Dihydroceramide Desaturase for Treating Disease. PCT Int. Appl. WO 2018112077, 2018.

(44). Mullen TD; Hannun YA; Obeid LM Ceramide synthases at the centre of sphingolipid metabolism and biology. Biochem. J 2012, 441, 789–802. [PubMed: 22248339]

(45). Levy M; Futerman AH Mammalian ceramide synthases. IUBMB Life 2010, 62, 347–356. [PubMed: 20222015]

(46). Car H; Zendzian-Piotrowska M; Prokopiuk S; Fiedorowicz A; Sadowska A; Kurek K; Sawicka D Ceramide profiles in the brain of rats with diabetes induced by streptozotocin. FEBS J 2012, 279, 1943–1952. [PubMed: 22429392]

(47). Brachtendorf S; El-Hindi K; Grosch S Ceramide synthases in cancer therapy and chemoresistance. Prog. Lipid Res 2019, 74, 160–185. [PubMed: 30953657]

(48). Wang E; Norred WP; Bacon CW; Riley RT; Merrill AH Jr. Inhibition of sphingolipid biosynthesis by fumonisins. Implications for diseases associated with fusarium moniliforme. J. Biol. Chem 1991, 266, 14486–14490. [PubMed: 1860857]

(49). Merrill AH Jr.; Sullards MC; Wang E; Voss KA; Riley RT Sphingolipid metabolism: Roles in signal transduction and disruption by fumonisins. Environ. Health Perspect 2001, 109 (Suppl.2), 283–289.

(50). Merrill AH Jr.; van Echten G; Wang E; Sandhoff K Fumonisin b1 inhibits sphingosine (sphinganine) n-acyltransferase and de novo sphingolipid biosynthesis in cultured neurons in situ. J. Biol. Chem 1993, 268, 27299–27306. [PubMed: 8262970]

(51). Humpf HU; Schmelz EM; Meredith FI; Vesper H; Vales TR; Wang E; Menaldino DS; Liotta DC; Merrill AH Jr. Acylation of naturally occurring and synthetic 1-deoxysphinganines by ceramide synthase. Formation of n-palmitoyl-aminopentol produces a toxic metabolite of hydrolyzed

fumonisin, ap1, and a new category of ceramide synthase inhibitor. J. Biol. Chem 1998, 273, 19060–19064. [PubMed: 9668088]

(52). Seiferlein M; Humpf HU; Voss KA; Sullards MC; Allegood JC; Wang E; Merrill AH Jr. Hydrolyzed fumonisins hfb1 and hfb2 are acylated in vitro and in vivo by ceramide synthase to form cytotoxic n-acyl-metabolites. Mol. Nutr. Food Res 2007, 51, 1120–1130. [PubMed: 17729221]

(53). Liu X; Fan L; Yin S; Chen H; Hu H Molecular mechanisms of fumonisin b1-induced toxicities and its applications in the mechanism-based interventions. Toxicon 2019, 167, 1–5. [PubMed: 31173793]

(54). Berdyshev EV; Gorshkova I; Skobeleva A; Bittman R; Lu X; Dudek SM; Mirzapoiazova T; Garcia JG; Natarajan V Fty720 inhibits ceramide synthases and up-regulates dihydrosphingosine 1-phosphate formation in human lung endothelial cells. J. Biol. Chem 2009, 284, 5467–5477. [PubMed: 19119142]

(55). Lahiri S; Park H; Laviad EL; Lu X; Bittman R; Futerman AH Ceramide synthesis is modulated by the sphingosine analog fty720 via a mixture of uncompetitive and noncompetitive inhibition in an acyl-coa chain length-dependent manner. J. Biol. Chem 2009, 284, 16090–16098. [PubMed: 19357080]

(56). Kim HJ; Qiao Q; Toop HD; Morris JC; Don AS A fluorescent assay for ceramide synthase activity. J. Lipid Res 2012, 53, 1701–1707. [PubMed: 22661289]

(57). Brinkmann V; Davis MD; Heise CE; Albert R; Cottens S; Hof R; Bruns C; Prieschl E; Baumruker T; Hiestand P; Foster CA; Zollinger M; Lynch KR The immune modulator fty720 targets sphingosine 1-phosphate receptors. J. Biol. Chem 2002, 277, 21453–21457. [PubMed: 11967257]

(58). Toop HD; Don AS; Morris JC Synthesis and biological evaluation of analogs of aal(s) for use as ceramide synthase 1 inhibitors. Org. Biomol. Chem 2015, 13, 11593–11596. [PubMed: 26535908]

(59). Schiffmann S; Hartmann D; Fuchs S; Birod K; Ferreiros N; Schreiber Y; Zivkovic A; Geisslinger G; Grosch S; Stark H Inhibitors of specific ceramide synthases. Biochimie 2012, 94, 558–565. [PubMed: 21945810]

(60). Turner N; Lim XY; Toop HD; Osborne B; Brandon AE; Taylor EN; Fiveash CE; Govindaraju H; Teo JD; McEwen HP; Couttas TA; Butler SM; Das A; Kowalski GM; Bruce CR; Hoehn KL; Fath T; Schmitz-Peiffer C; Cooney GJ; Montgomery MK; Morris JC; Don AS A selective inhibitor of ceramide synthase 1 reveals a novel role in fat metabolism. Nat. Commun 2018, 9, 3165. [PubMed: 30131496]

(61). Fanani ML; Maggio B The many faces (and phases) of ceramide and sphingomyelin i - single lipids. Biophys. Rev 2017, 9, 589–600. [PubMed: 28815463]

(62). Fanani ML; Maggio B The many faces (and phases) of ceramide and sphingomyelin ii - binary mixtures. Biophys. Rev 2017, 9, 601–616. [PubMed: 28823080]

(63). van Meer G Lipid traffic in animal cells. Annu. Rev. Cell Biol 1989, 5, 247–275. [PubMed: 2688705]

(64). Goni FM; Alonso A Sphingomyelinases: Enzymology and membrane activity. FEBS Lett 2002, 531, 38–46. [PubMed: 12401200]

(65). Schuchman EH; Desnick RJ Types a and b niemann-pick disease. Mol. Genet. Metab 2017, 120, 27–33. [PubMed: 28164782]

(66). Gorelik A; Illes K; Heinz LX; Superti-Furga G; Nagar B Crystal structure of mammalian acid sphingomyelinase. Nat. Commun 2016, 7, 12196. [PubMed: 27435900]

(67). Xiong ZJ; Huang J; Poda G; Pomes R; Prive GG Structure of human acid sphingomyelinase reveals the role of the saposin domain in activating substrate hydrolysis. J. Mol. Biol 2016, 428, 3026–3042. [PubMed: 27349982]

(68). Zhou YF; Metcalf MC; Garman SC; Edmunds T; Qiu H; Wei RR Human acid sphingomyelinase structures provide insight to molecular basis of niemann-pick disease. Nat. Commun 2016, 7, 13082. [PubMed: 27725636]

(69). Igarashi M; Suzuki K; Chen SM; Suzuki K Changes in brain hydrolytic enzyme activities in rats treated with cholesterol biosynthesis inhibitor, ay9944. Brain Res 1975, 90, 97–114. [PubMed: 48406]

(70). Sakuragawa M Niemann-pick disease-like inclusions caused by a hypocholesteremic agent. Invest. Ophthalmol 1976, 15, 1022–1027. [PubMed: 62729]

(71). Sakuragawa N; Sakuragaw M; Kuwabara T; Pentchev PG; Barranger JA; Brady RO Niemann-pick disease experimental model: Sphingomyelinase reduction induced by ay-9944. Science 1977, 196, 317–319. [PubMed: 66749]

(72). Albouz S; Hauw JJ; Berwald-Netter Y; Boutry JM; Bourdon R; Baumann N Tricyclic antidepressants induce sphingomyelinase deficiency in fibroblast and neuroblastoma cell cultures. Biomedicine 1981, 35, 218–220. [PubMed: 6285997]

(73). Yoshida Y; Arimoto K; Sato M; Sakuragawa N; Arima M; Satoyoshi E Reduction of acid sphingomyelinase activity in human fibroblasts induced by ay-9944 and other cationic amphiphilic drugs. J. Biochem 1985, 98, 1669–1679. [PubMed: 2419314]

(74). Masson M; Albouz S; Boutry JM; Spezzatti B; Castagna M; Baumann N Calmodulin antagonist w-7 inhibits lysosomal sphingomyelinase activity in c6 glioma cells. J. Neurochem 1989, 52, 1645–1647. [PubMed: 2540282]

(75). Jaffrezou JP; Herbert JM; Levade T; Gau MN; Chatelain P; Laurent G Reversal of multidrug resistance by calcium channel blocker sr33557 without photoaffinity labeling of p-glycoprotein. J. Biol. Chem 1991, 266, 19858–19864. [PubMed: 1918089]

(76). Kornhuber J; Tripal P; Reichel M; Terfloth L; Bleich S; Wiltfang J; Gulbins E Identification of new functional inhibitors of acid sphingomyelinase using a structure-property-activity relation model. J. Med. Chem 2008, 51, 219–237. [PubMed: 18027916]

(77). Kolzer M; Werth N; Sandhoff K Interactions of acid sphingomyelinase and lipid bilayers in the presence of the tricyclic antidepressant desipramine. FEBS Lett 2004, 559, 96–98. [PubMed: 14960314]

(78). Kornhuber J; Tripal P; Reichel M; Muhle C; Rhein C; Muehlbacher M; Groemer TW; Gulbins E Functional inhibitors of acid sphingomyelinase (fiasmas): A novel pharmacological group of drugs with broad clinical applications. Cell. Physiol. Biochem 2010, 26, 9–20. [PubMed: 20502000]

(79). Adams C; Icheva V; Deppisch C; Lauer J; Herrmann G; Graepler-Mainka U; Heyder S; Gulbins E; Riethmueller J Longterm pulmonal therapy of cystic fibrosis-patients with amitriptyline. Cell. Physiol. Biochem 2016, 39, 565–572. [PubMed: 27395380]

(80). Okudaira C; Ikeda Y; Kondo S; Furuya S; Hirabayashi Y; Koyano T; Saito Y; Umezawa K Inhibition of acidic sphingomyelinase by xanthone compounds isolated from garcinia speciosa. J. Enzyme Inhib 2000, 15, 129–138. [PubMed: 10938539]

(81). Wetzel S; Wilk W; Chammaa S; Sperl B; Roth AG; Yektaoglu A; Renner S; Berg T; Arenz C; Giannis A; Oprea TI; Rauh D; Kaiser M; Waldmann H A scaffold-tree-merging strategy for prospective bioactivity annotation of gamma-pyrones. Angew. Chem., Int. Ed 2010, 49, 3666–3670.

(82). Kobayashi K; Ishizaki Y; Kojo S; Kikuzaki H Strong inhibition of secretory sphingomyelinase by catechins, particularly by (−)-epicatechin 3-o-gallate and (−)-3′-o-methylepigallocatechin 3-o-gallate. J. Nutr. Sci. Vitaminol 2016, 62, 123–129. [PubMed: 27264097]

(83). Quintern LE; Weitz G; Nehrkorn H; Tager JM; Schram AW; Sandhoff K Acid sphingomyelinase from human urine: Purification and characterization. Biochim. Biophys. Acta, Lipids Lipid Metab 1987, 922, 323–336.

(84). Kolzer M; Arenz C; Ferlinz K; Werth N; Schulze H; Klingenstein R; Sandhoff K Phosphatidylinositol-3,5-bisphosphate is a potent and selective inhibitor of acid sphingomyelinase. Biol. Chem 2003, 384, 1293–1298. [PubMed: 14515991]

(85). Roth AG; Redmer S; Arenz C Potent inhibition of acid sphingomyelinase by phosphoinositide analogues. ChemBioChem 2009, 10, 2367–2374. [PubMed: 19688786]

(86). Roth AG; Drescher D; Yang Y; Redmer S; Uhlig S; Arenz C Potent and selective inhibition of acid sphingomyelinase by bisphosphonates. Angew. Chem., Int. Ed 2009, 48, 7560–7563.

(87). Bae J-S; Jin HK; Park MH 2-Amino-2-(1,2,3-triazole-4-yl)propane-1,3-diol Derivative of Novel Compound for Directly Inhibiting ASM Activity, and Use Thereof. PCT Int. Appl. WO 2019/212196, 2019.

(88). Yang K; Nong K; Gu Q; Dong J; Wang J Discovery of n-hydroxy-3-alkoxybenzamides as direct acid sphingomyelinase inhibitors using a ligand-based pharmacophore model. Eur. J. Med. Chem 2018, 151, 389–400. [PubMed: 29649738]

(89). Yang K; Yu J; Nong K; Wang Y; Niu A; Chen W; Dong J; Wang J Discovery of potent, selective, and direct acid sphingomyelinase inhibitors with antidepressant activity. J. Med. Chem 2020, 63, 961–974. [PubMed: 31944697]

(90). Tomiuk S; Hofmann K; Nix M; Zumbansen M; Stoffel W Cloned mammalian neutral sphingomyelinase: Functions in sphingolipid signaling? Proc. Natl. Acad. Sci. U. S. A 1998, 95, 3638–3643. [PubMed: 9520418]

(91). Hofmann K; Tomiuk S; Wolff G; Stoffel W Cloning and characterization of the mammalian brain-specific, mg2+-dependent neutral sphingomyelinase. Proc. Natl. Acad. Sci. U. S. A 2000, 97, 5895–5900. [PubMed: 10823942]

(92). Krut O; Wiegmann K; Kashkar H; Yazdanpanah B; Kronke M Novel tumor necrosis factor-responsive mammalian neutral sphingomyelinase-3 is a c-tail-anchored protein. J. Biol. Chem 2006, 281, 13784–13793. [PubMed: 16517606]

(93). Wu BX; Rajagopalan V; Roddy PL; Clarke CJ; Hannun YA Identification and characterization of murine mitochondria-associated neutral sphingomyelinase (ma-nsmase), the mammalian sphingomyelin phosphodiesterase 5. J. Biol. Chem 2010, 285, 17993–18002. [PubMed: 20378533]

(94). Clarke CJ; Snook CF; Tani M; Matmati N; Marchesini N; Hannun YA The extended family of neutral sphingomyelinases. Biochemistry 2006, 45, 11247–11256. [PubMed: 16981685]

(95). Wu BX; Clarke CJ; Hannun YA Mammalian neutral sphingomyelinases: Regulation and roles in cell signaling responses. NeuroMol. Med 2010, 12, 320–330.

(96). Airola MV; Shanbhogue P; Shamseddine AA; Guja KE; Senkal CE; Maini R; Bartke N; Wu BX; Obeid LM; Garcia-Diaz M; Hannun YA Structure of human nsmase2 reveals an interdomain allosteric activation mechanism for ceramide generation. Proc. Natl. Acad. Sci. U. S. A 2017, 114, E5549–E5558. [PubMed: 28652336]

(97). Shanbhogue P; Hoffmann RM; Airola MV; Maini R; Hamelin DJ; Garcia-Diaz M; Burke JE; Hannun YA The juxtamembrane linker in neutral sphingomyelinase-2 functions as an intramolecular allosteric switch that activates the enzyme. J. Biol. Chem 2019, 294, 7488–7502. [PubMed: 30890560]

(98). Nara F; Tanaka M; Hosoya T; Suzuki-Konagai K; Ogita T Scyphostatin, a neutral sphingomyelinase inhibitor from a discomycete, trichopeziza mollissima: Taxonomy of the producing organism, fermentation, isolation, and physico-chemical properties. J. Antibiot 1999, 52, 525–530.

(99). Tanaka M; Nara F; Suzuki-Konagai K; Hosoya T; Ogita T Structural elucidation of scyphostatin, an inhibitor of membrane-bound neutral sphingomyelinase. J. Am. Chem. Soc 1997, 119, 7871–7872.

(100). Ghosh P; Chatterjee S Effects of gentamicin on sphingomyelinase activity in cultured human renal proximal tubular cells. J. Biol. Chem 1987, 262, 12550–12556. [PubMed: 3040755]

(101). Lister MD; Crawford-Redick CL; Loomis CR Characterization of the neutral ph-optimum sphingomyelinase from rat brain: Inhibition by copper ii and ganglioside gm3. Biochim. Biophys. Acta, Lipids Lipid Metab 1993, 1165, 314–320.

(102). Nara F; Tanaka M; Masuda-Inoue S; Yamasato Y; Doi-Yoshioka H; Suzuki-Konagai K; Kumakura S; Ogita T Biological activities of scyphostatin, a neutral sphingomyelinase inhibitor from a discomycete, trichopeziza mollissima. J. Antibiot 1999, 52, 531–535.

(103). Arenz C; Giannis A Synthesis of the first selective irreversible inhibitor of neutral sphingomyelinase. Angew. Chem., Int. Ed 2000, 39, 1440–1442.

(104). Arenz C; Gartner M; Waschołowski V; Giannis A Synthesis and biochemical investigation of scyphostatin analogues as inhibitors of neutral sphingomyelinase. Bioorg. Med. Chem 2001, 9, 2901–2904. [PubMed: 11597471]

(105). Arenz C; Thutewohl M; Block O; Waldmann H; Altenbach HJ; Giannis A Manumycin a and its analogues are irreversible inhibitors of neutral sphingomyelinase. ChemBioChem 2001, 2, 141–143. [PubMed: 11828438]

(106). Uchida R; Tomoda H; Dong Y; Omura S Alutenusin, a specific neutral sphingomyelinase inhibitor, produced by penicillium sp. Fo-7436. J. Antibiot 1999, 52, 572–574.

(107). Tanaka M; Nara F; Yamasato Y; Ono Y; Ogita T F-11334s, new inhibitors of membrane-bound neutral sphingomyelinase. J. Antibiot 1999, 52, 827–830.

(108). Ogura Y; Nara F; Hosoya T New Compound F-11263. Jpn. Pat. Appl. JPH0853387, 1996.

(109). Martin SF; Navarro F; Forthoffer N; Navas P; Villalba JM Neutral magnesium-dependent sphingomyelinase from liver plasma membrane: Purification and inhibition by ubiquinol. J. Bioenerg. Biomembr 2001, 33, 143–153. [PubMed: 11456220]

(110). Martin SF; Gomez-Diaz C; Navas P; Villalba JM Ubiquinol inhibition of neutral sphingomyelinase in liver plasma membrane: Specific inhibition of the mg(2+)-dependent enzyme and role of isoprenoid chain. Biochem. Biophys. Res. Commun 2002, 297, 581–586. [PubMed: 12270134]

(111). Lister MD; Ruan ZS; Bittman R Interaction of sphingomyelinase with sphingomyelin analogs modified at the c-1 and c-3 positions of the sphingosine backbone. Biochim. Biophys. Acta, Lipids Lipid Metab 1995, 1256, 25–30.

(112). Yokomatsu T; Takechi H; Akiyama T; Shibuya S; Kominato T; Soeda S; Shimeno H Synthesis and evaluation of a difluoromethylene analogue of sphingomyelin as an inhibitor of sphingomyelinase. Bioorg. Med. Chem. Lett 2001, 11, 1277–1280. [PubMed: 11392536]

(113). Yokomatsu T; Murano T; Akiyama T; Koizumi J; Shibuya S; Tsuji Y; Soeda S; Shimeno H Synthesis of non-competitive inhibitors of sphingomyelinases with significant activity. Bioorg. Med. Chem. Lett 2003, 13, 229–236. [PubMed: 12482429]

(114). Taguchi M; Sugimoto K; Goda K; Akama T; Yamamoto K; Suzuki T; Tomishima Y; Nishiguchi M; Arai K; Takahashi K; Kobori T Sphingomyelin analogues as inhibitors of sphingomyelinase. Bioorg. Med. Chem. Lett 2003, 13, 1963–1966. [PubMed: 12781174]

(115). Jung SM; Jeong EM; Jo DH; Chin MR; Jun HJ; Kim YH; Jeon HJ; Lee DH; Park MJ; Oh MJ; Yim CB; Kim DK Inhibition of a neutral form of sphingomyelinase by alkylthioureido-l,3-propandiols, ky353x series. J. Appl. Pharmacol 2003, 11, 169–173.

(116). Wascholowski V; Giannis A Sphingolactones: Selective and irreversible inhibitors of neutral sphingomyelinase. Angew. Chem., Int. Ed 2006, 45, 827–830.

(117). Amtmann E; Zoller M; Schilling G Neutral sphingomyelinase-inhibiting guanidines prevent herpes simplex virus-1 replication. Drugs Exp Clin Res 2000, 26, 57–65. [PubMed: 10894556]

(118). Amtmann E; Baader W; Zoller M Neutral sphingomyelinase inhibitor c11ag prevents lipopolysaccharide-induced macrophage activation. Drugs Exp. Clin. Res 2003, 29, 5–13. [PubMed: 12866359]

(119). Collenburg L; Beyersdorf N; Wiese T; Arenz C; Saied EM; Becker-Flegler KA; Schneider-Schaulies S; Avota E The activity of the neutral sphingomyelinase is important in T cell recruitment and directional migration. Front. Immunol 2017, 8, 1007. [PubMed: 28871263]

(120). Wachter MP; Lalan P Substituted Amino Acids as Neutral Sphingomyelinase Inhibitors. PCT Int. Appl. WO 2001/056560, 2001.

(121). Luberto C; Hassler DF; Signorelli P; Okamoto Y; Sawai H; Boros E; Hazen-Martin DJ; Obeid LM; Hannun YA; Smith GK Inhibition of tumor necrosis factor-induced cell death in mcf7 by a novel inhibitor of neutral sphingomyelinase. J. Biol. Chem 2002, 277, 41128–41139. [PubMed: 12154098]

(122). Tamiya-Koizumi K; Kojima K Activation of magnesium-dependent, neutral sphingomyelinase by phosphatidylserine. J. Biochem 1986, 99, 1803–1806. [PubMed: 3017927]

(123). Dinkins MB; Dasgupta S; Wang G; Zhu G; Bieberich E Exosome reduction in vivo is associated with lower amyloid plaque load in the 5xfad mouse model of Alzheimer's disease. Neurobiol. Aging 2014, 35, 1792–1800. [PubMed: 24650793]

(124). Asai H; Ikezu S; Tsunoda S; Medalla M; Luebke J; Haydar T; Wolozin B; Butovsky O; Kugler S; Ikezu T Depletion of microglia and inhibition of exosome synthesis halt tau propagation. Nat. Neurosci 2015, 18, 1584–1593. [PubMed: 26436904]

(125). Kumar A; Henry RJ; Stoica BA; Loane DJ; Abulwerdi G; Bhat SA; Faden AI Neutral sphingomyelinase inhibition alleviates lps-induced microglia activation and neuroinflammation after experimental traumatic brain injury. J. Pharmacol. Exp. Ther 2019, 368, 338–352. [PubMed: 30563941]

(126). Okuro RT; Machado MN; Casquilho NV; Jardim-Neto A; Roncally-Carvalho A; Atella GC; Zin WA The role of sphingolipid metabolism disruption on lipopolysaccharide-induced lung injury in mice. Pulm. Pharmacol. Ther 2018, 50, 100–110. [PubMed: 29702255]

(127). Lallemand T; Rouahi M; Swiader A; Grazide MH; Geoffre N; Alayrac P; Recazens E; Coste A; Salvayre R; Negre-Salvayre A; Auge N Nsmase2 (type 2-neutral sphingomyelinase) deficiency or inhibition by gw4869 reduces inflammation and atherosclerosis in apoe(−/−) mice. Arterioscler., Thromb., Vasc. Biol 2018, 38, 1479–1492. [PubMed: 29794115]

(128). Coblentz PD; Ahn B; Hayward LF; Yoo JK; Christou DD; Ferreira LF Small-hairpin rna and pharmacological targeting of neutral sphingomyelinase prevent diaphragm weakness in rats with heart failure and reduced ejection fraction. Am. J. Physiol Lung Cell Mol. Physiol 2019, 316, L679–L690. [PubMed: 30702345]

(129). Huang L; Hu C; Chao H; Zhang Y; Li Y; Hou J; Xu Z; Lu H; Li H; Chen H Drug-resistant endothelial cells facilitate progression, emt and chemoresistance in nasopharyngeal carcinoma via exosomes. Cell. Signalling 2019, 63, 109385. [PubMed: 31394194]

(130). Wang B; Wang Y; Yan Z; Sun Y; Su C Colorectal cancer cell-derived exosomes promote proliferation and decrease apoptosis by activating the erk pathway. Int. J. Clin. Exp. Pathol 2019, 12, 2485–2495. [PubMed: 31934075]

(131). Delaet N; Ohmawari N; Nakai H 4H-1,2,4-Triazole-3(2H)-thione Deratives as Sphingomyelinase Inhibitors. PCT Int. Appl. WO 2002/066447, 2002.

(132). Heltweg B; Gatbonton T; Schuler AD; Posakony J; Li H; Goehle S; Kollipara R; Depinho RA; Gu Y; Simon JA; Bedalov A Antitumor activity of a small-molecule inhibitor of human silent information regulator 2 enzymes. Cancer Res 2006, 66, 4368–4377. [PubMed: 16618762]

(133). Figuera-Losada M; Stathis M; Dorskind JM; Thomas AG; Bandaru VV; Yoo SW; Westwood NJ; Rogers GW; McArthur JC; Haughey NJ; Slusher BS; Rojas C Cambinol, a novel inhibitor of neutral sphingomyelinase 2 shows neuroprotective properties. PLoS One 2015, 10, No. e0124481.

(134). Bilousova T; Elias C; Miyoshi E; Alam MP; Zhu C; Campagna J; Vadivel K; Jagodzinska B; Gylys KH; John V Suppression of tau propagation using an inhibitor that targets the dk-switch of nsmase2. Biochem. Biophys. Res. Commun 2018, 499, 751–757. [PubMed: 29604274]

(135). Rojas C; Barnaeva E; Thomas AG; Hu X; Southall N; Marugan J; Chaudhuri AD; Yoo SW; Hin N; Stepanek O; Wu Y; Zimmermann SC; Gadiano AG; Tsukamoto T; Rais R; Haughey N; Ferrer M; Slusher BS Dptip, a newly identified potent brain penetrant neutral sphingomyelinase 2 inhibitor, regulates astrocyte-peripheral immune communication following brain inflammation. Sci. Rep 2018, 8, 17715. [PubMed: 30531925]

(136). Stepanek O; Hin N; Thomas AG; Dash RP; Alt J; Rais R; Rojas C; Slusher BS; Tsukamoto T Neutral sphingomyelinase 2 inhibitors based on the 4-(1h-imidazol-2-yl)-2,6-dialkoxyphenol scaffold. Eur. J. Med. Chem 2019, 170, 276–289. [PubMed: 30921693]

(137). Rojas C; Sala M; Thomas AG; Datta Chaudhuri A; Yoo SW; Li Z; Dash RP; Rais R; Haughey NJ; Nencka R; Slusher B A novel and potent brain penetrant inhibitor of extracellular vesicle release. Br. J. Pharmacol 2019, 176, 3857–3870. [PubMed: 31273753]

(138). Sala M; Hollinger KR; Thomas AG; Dash RP; Tallon C; Veeravalli V; Lovell L; Kogler M; Hrebabecky H; Prochazkova E; Nesuta O; Donoghue A; Lam J; Rais R; Rojas C; Slusher BS; Nencka R Novel human neutral sphingomyelinase 2 inhibitors as potential therapeutics for alzheimer's disease. J. Med. Chem 2020, 63, 6028–6056.

(139). Bilousova T; Simmons BJ; Knapp RR; Elias CJ; Campagna J; Melnik M; Chandra S; Focht S; Zhu C; Vadivel K; Jagodzinska B; Cohn W; Spilman P; Gylys KH; Garg NK; John V Dual neutral sphingomyelinase-2/acetylcholinesterase inhibitors for the treatment of Alzheimer's disease. ACS Chem. Biol 2020, 15, 1671–1684. [PubMed: 32352753]

(140). Yu Q.-s.; Liu C; Brzostowska M; Chrisey L; Brossi A; Greig NH; Atack JR; Soncrant TT; Rapoport SI; Radunz H-E Physovenines: Efficient synthesis of (−)- and (+)-physovenine and

synthesis of carbarnate analogues of (−)-physovenine. Anticholinesterase activity and analgesic properties of optically active physovenines. Helv. Chim. Acta 1991, 74, 761–766.

(141). Oda M; Hashimoto M; Takahashi M; Ohmae Y; Seike S; Kato R; Fujita A; Tsuge H; Nagahama M; Ochi S; Sasahara T; Hayashi S; Hirai Y; Sakurai J Role of sphingomyelinase in infectious diseases caused by bacillus cereus. PLoS One 2012, 7, No. e38054.

(142). Openshaw AE; Race PR; Monzo HJ; Vazquez-Boland JA; Banfield MJ Crystal structure of smcl, a bacterial neutral sphingomyelinase c from listeria. J. Biol. Chem 2005, 280, 35011–35017. [PubMed: 16093240]

(143). Ago H; Oda M; Takahashi M; Tsuge H; Ochi S; Katunuma N; Miyano M; Sakurai J Structural basis of the sphingomyelin phosphodiesterase activity in neutral sphingomyelinase from bacillus cereus. J. Biol. Chem 2006, 281, 16157–16167. [PubMed: 16595670]

(144). Huseby M; Shi K; Brown CK; Digre J; Mengistu F; Seo KS; Bohach GA; Schlievert PM; Ohlendorf DH; Earhart CA Structure and biological activities of beta toxin from staphylococcus aureus. J. Bacteriol 2007, 189, 8719–8726. [PubMed: 17873030]

(145). Kruse AC; Huseby MJ; Shi K; Digre J; Ohlendorf DH; Earhart CA Structure of a mutant beta toxin from staphylococcus aureus reveals domain swapping and conformational flexibility. Acta Crystallogr., Sect. F: Struct. Biol. Cryst. Commun 2011, 67, 438–441.

(146). Hakogi T; Monden Y; Iwama S; Katsumura S Stereo-controlled synthesis of a sphingomyelin methylene analogue as a sphingomyelinase inhibitor. Org. Lett 2000, 2, 2627–2629. [PubMed: 10990413]

(147). Hakogi T; Monden Y; Taichi M; Iwama S; Fujii S; Ikeda K; Katsumura S Synthesis of sphingomyelin carbon analogues as sphingomyelinase inhibitors. J. Org. Chem 2002, 67, 4839–4846. [PubMed: 12098296]

(148). Hakogi T; Taichi M; Katsumura S Synthesis of a nitrogen analogue of sphingomyelin as a sphingomyelinase inhibitor. Org. Lett 2003, 5, 2801–2804. [PubMed: 12889878]

(149). Hakogi T; Yamamoto T; Fujii S; Ikeda K; Katsumura S Synthesis of sphingomyelin difluoromethylene analogue. Tetrahedron Lett 2006, 47, 2627–2630.

(150). Hakogi T; Fujii S; Morita M; Ikeda K; Katsumura S Synthesis of sphingomyelin sulfur analogue and its behavior toward sphingomyelinase. Bioorg. Med. Chem. Lett 2005, 15, 2141–2144. [PubMed: 15808485]

(151). Imagawa H; Oda M; Takemoto T; Yamauchi R; Yoshikawa T; Yamamoto H; Nishizawa M; Takahashi H; Hashimoto M; Yabiku K; Nagahama M; Sakurai J Synthesis and evaluation of novel phosphate ester analogs as neutral sphingomyelinase inhibitors. Bioorg. Med. Chem. Lett 2010, 20, 3868–3871. [PubMed: 20627555]

(152). Oda M; Imagawa H; Kato R; Yabiku K; Yoshikawa T; Takemoto T; Takahashi H; Yamamoto H; Nishizawa M; Sakurai J; Nagahama M Novel inhibitor of bacterial sphingomyelinase, smy-540, developed based on three-dimensional structure analysis. J. Enzyme Inhib. Med. Chem 2014, 29, 303–310. [PubMed: 23488740]

(153). Waggoner DW; Gomez-Munoz A; Dewald J; Brindley DN Phosphatidate phosphohydrolase catalyzes the hydrolysis of ceramide 1-phosphate, lysophosphatidate, and sphingosine 1-phosphate. J. Biol. Chem 1996, 271, 16506–16509. [PubMed: 8663293]

(154). Shinghal R; Scheller RH; Bajjalieh SM Ceramide 1-phosphate phosphatase activity in brain. J. Neurochem 1993, 61, 2279–2285. [PubMed: 8245978]

(155). Boudker O; Futerman AH Detection and characterization of ceramide-1-phosphate phosphatase activity in rat liver plasma membrane. J. Biol. Chem 1993, 268, 22150–22155. [PubMed: 8408075]

(156). Stirnemann J; Belmatoug N; Camou F; Serratrice C; Froissart R; Caillaud C; Levade T; Astudillo L; Serratrice J; Brassier A; Rose C; Billette de Villemeur T; Berger MG A review of gaucher disease pathophysiology, clinical presentation and treatments. Int. J. Mol. Sci 2017, 18, 441.

(157). Won JS; Singh AK; Singh I Biochemical, cell biological, pathological, and therapeutic aspects of Krabbe's disease. J. Neurosci. Res 2016, 94, 990–1006. [PubMed: 27638584]

(158). Maegawa GH; Tropak MB; Buttner JD; Rigat BA; Fuller M; Pandit D; Tang L; Kornhaber GJ; Hamuro Y; Clarke JT; Mahuran DJ Identification and characterization of ambroxol as an enzyme

enhancement agent for gaucher disease. J. Biol. Chem 2009, 284, 23502–23516. [PubMed: 19578116]

(159). Boyd RE; Lee G; Rybczynski P; Benjamin ER; Khanna R; Wustman BA; Valenzano KJ Pharmacological chaperones as therapeutics for lysosomal storage diseases. J. Med. Chem 2013, 56, 2705–2725. [PubMed: 23363020]

(160). Arenz C Recent advances and novel treatments for sphingolipidoses. Future Med. Chem 2017, 9, 1687–1700. [PubMed: 28857617]

(161). Chew WS; Seow WL; Chong JR; Lai MKP; Torta F; Wenk MR; Herr DR Sphingolipidomics analysis of large clinical cohorts. Part 1: Technical notes and practical considerations. Biochem. Biophys. Res. Commun 2018, 504, 596–601. [PubMed: 29654754]

(162). Chong JR; Xiang P; Wang W; Hind T; Chew WS; Ong WY; Lai MKP; Herr DR Sphingolipidomics analysis of large clinical cohorts. Part 2: Potential impact and applications. Biochem. Biophys. Res. Commun 2018, 504, 602–607. [PubMed: 29654757]

(163). Matanes F; Twal WO; Hammad SM Sphingolipids as biomarkers of disease. Adv. Exp. Med. Biol 2019, 1159, 109–138. [PubMed: 31502202]

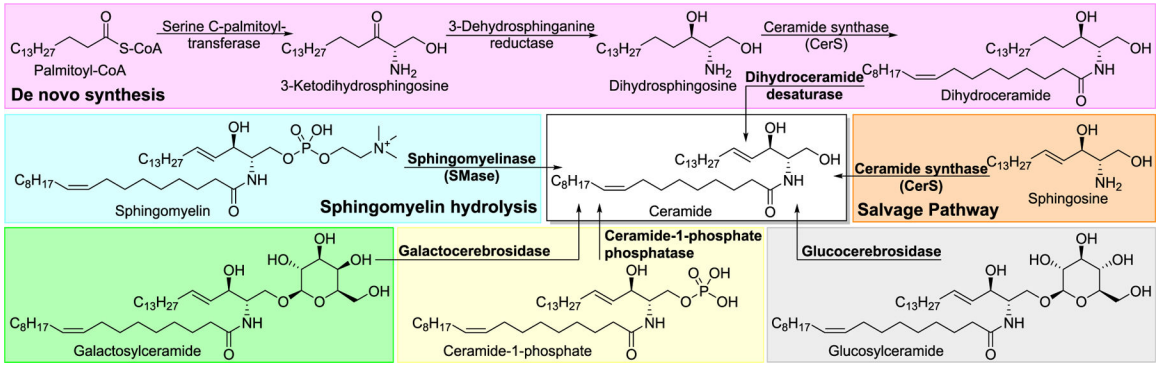

Figure 1.

Ceramide biosynthesis pathways (adapted from ref 5). Various biosynthetic routes to ceramide are depicted for Cer(d18:1/18:1(9Z)). De novo pathway, salvage pathway, and sphingomyelin hydrolysis are highlighted in purple, orange, and cyan, respectively. Other sources of ceramide include glucocerebrosidase (gray), galactocerebrosidase (green), and ceramide-1-phosphate phosphatase (beige).

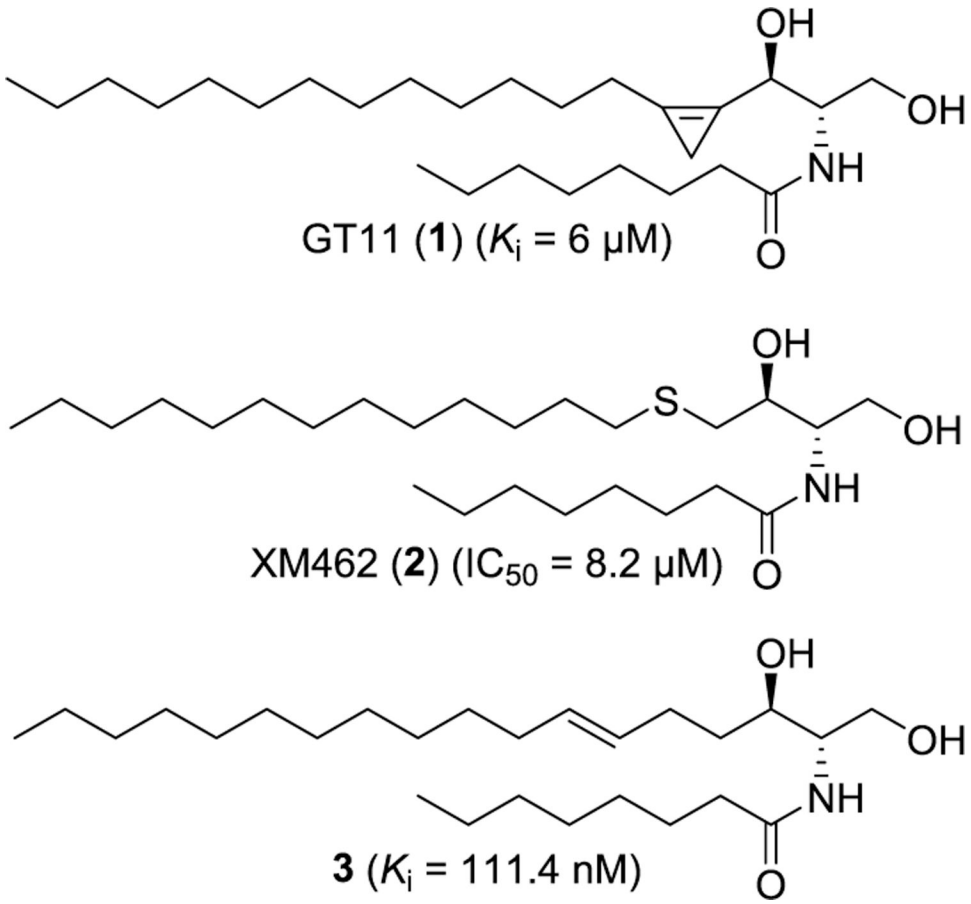

Figure 2.
Structures of ceramide-based DES1 inhibitors GT11 (**1**), XM462 (**2**), and compound **3**.

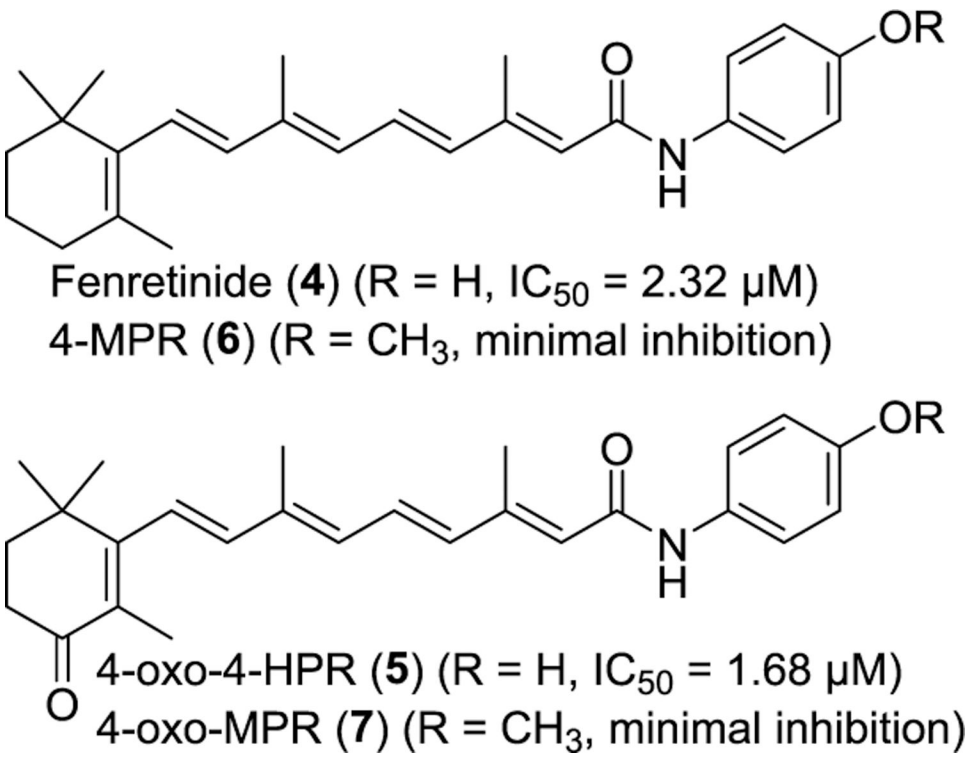

Figure 3.
Structures of retinoid-based DES1 inhibitors **4–7**.

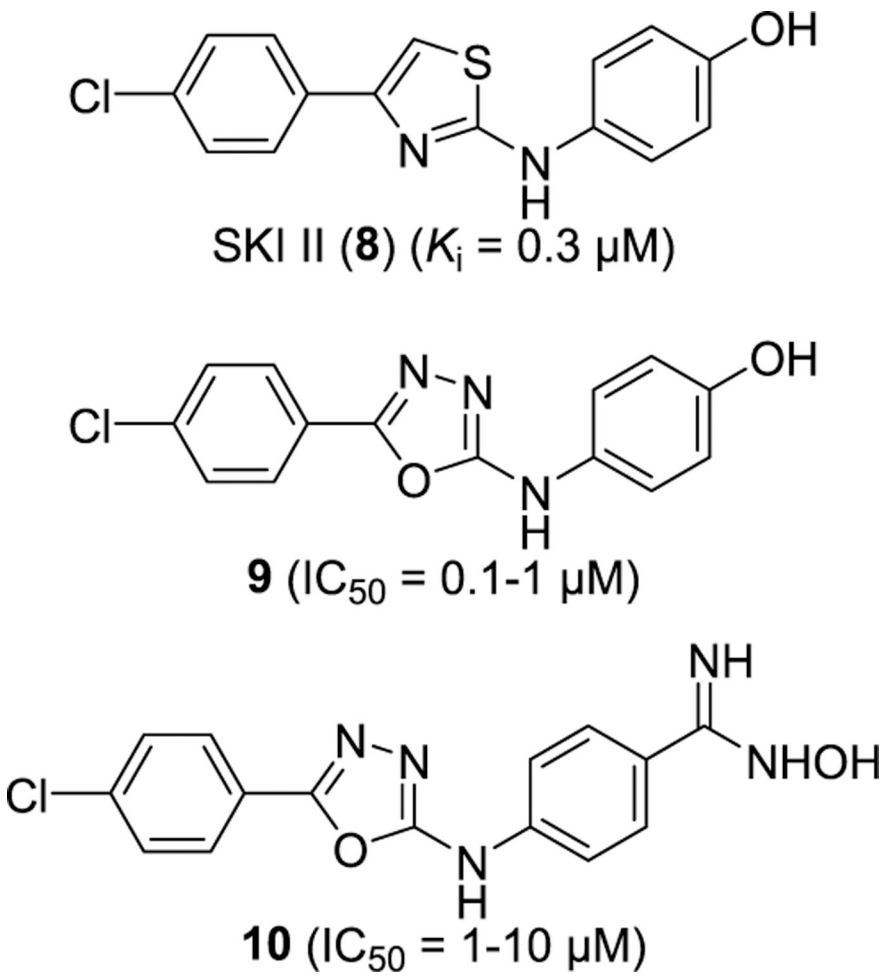

Figure 4.
Structures of SKI II (**8**) and its derivatives **9** and **10**.

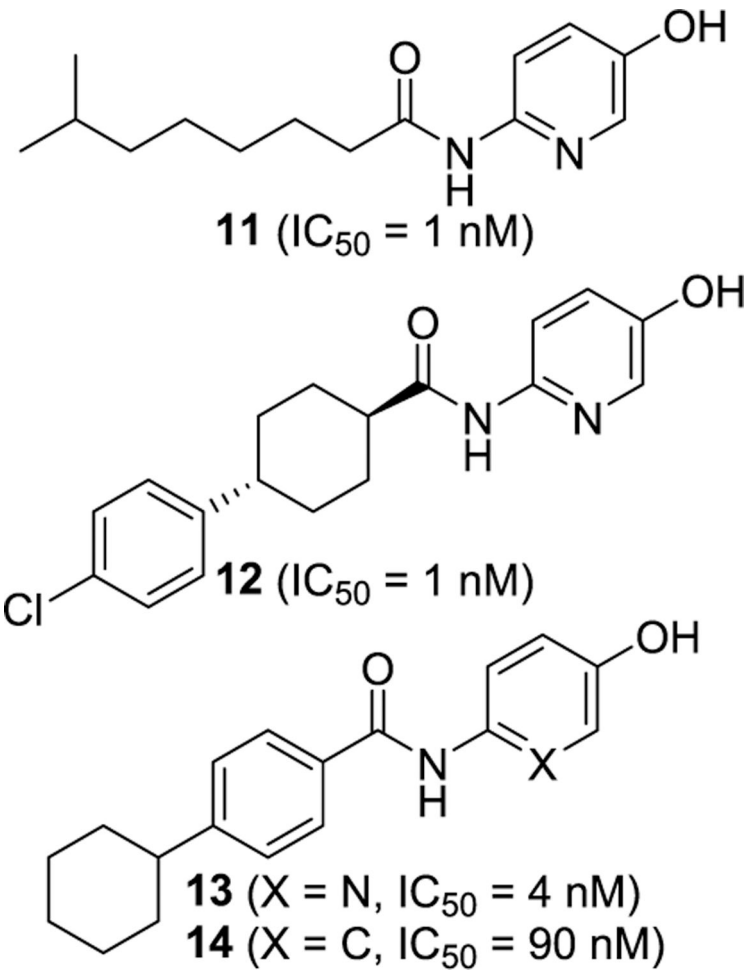

Figure 5.
Structures of DES1 inhibitors **11–14** containing a 6-acylamino-3-pyridinol or 4-acylaminophenol scaffold.

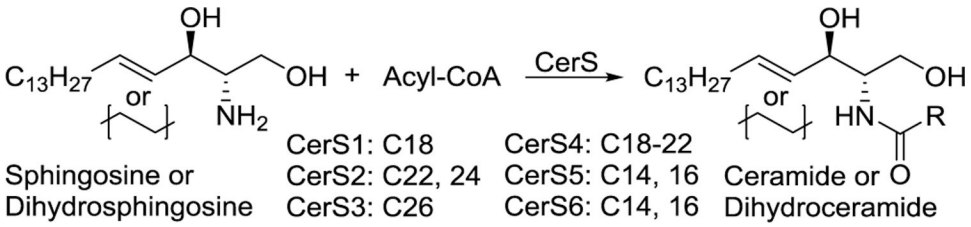

Figure 6.

Acyl-CoA substrate preference of CerS isoforms.[10]

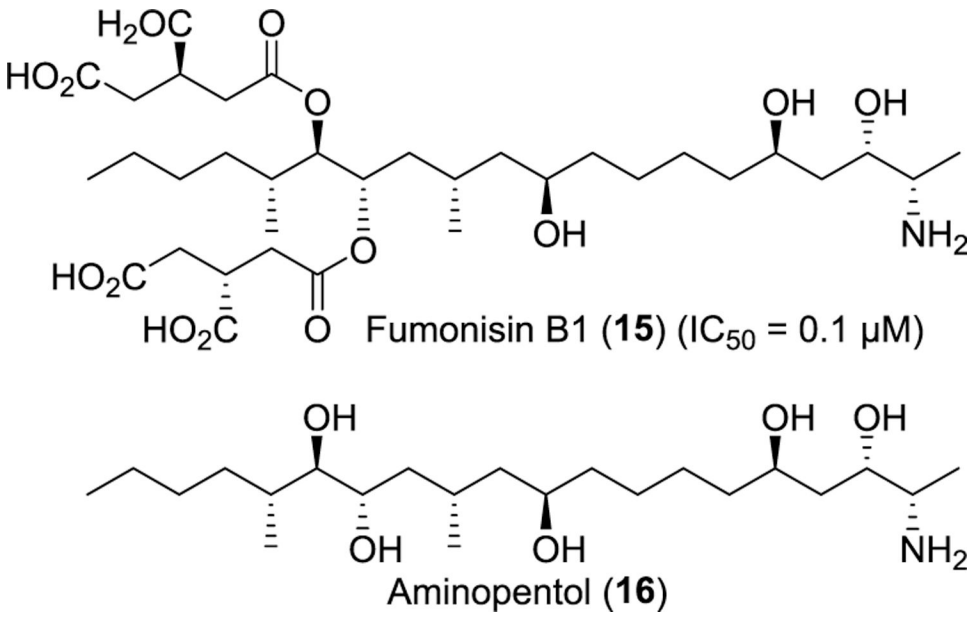

Figure 7.
Structures of fumonisin B1 (**15**) and aminopentol (**16**).

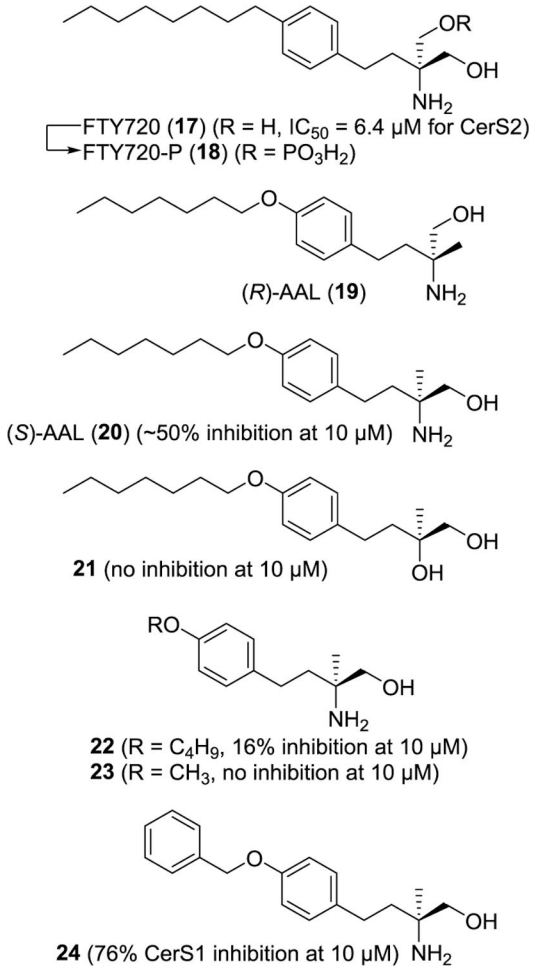

Figure 8.
Structures of FTY720 (**17**) and its derivatives **18–24**.

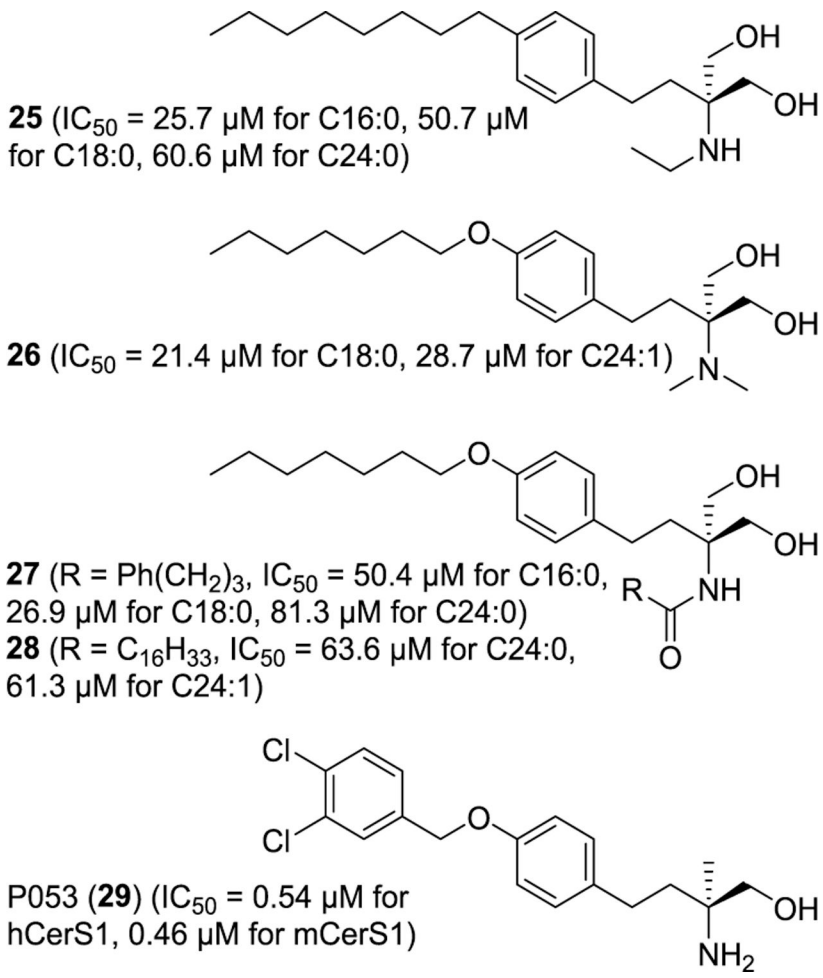

Figure 9.
Structures of CerS inhibitors **25–29** derived from FTY720 (**17**).

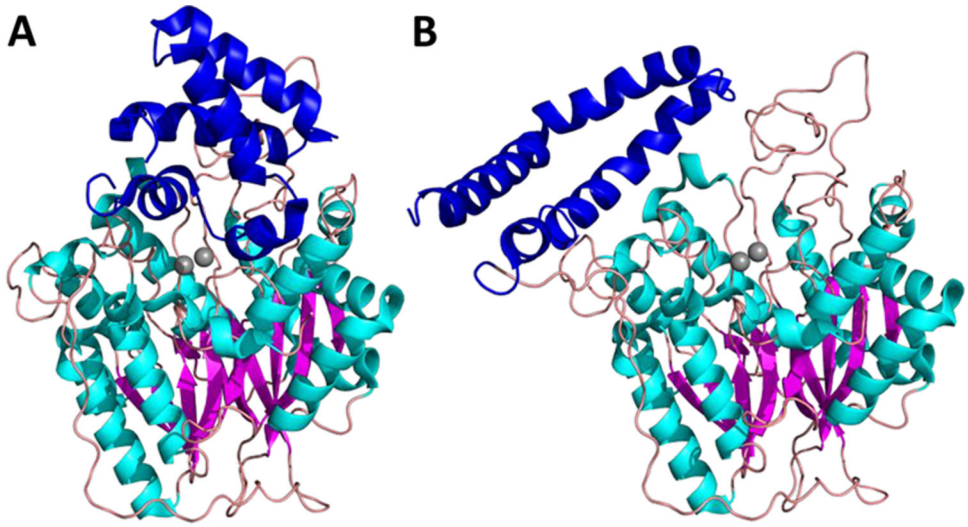

Figure 10.

Crystal structures of (A) the closed form (PDB code 5FI9) and (B) the open form (PDB code 5FIB) of murine aSMase.[66] The saposin domain is shown in blue, and the active site zinc ions are shown as gray spheres.

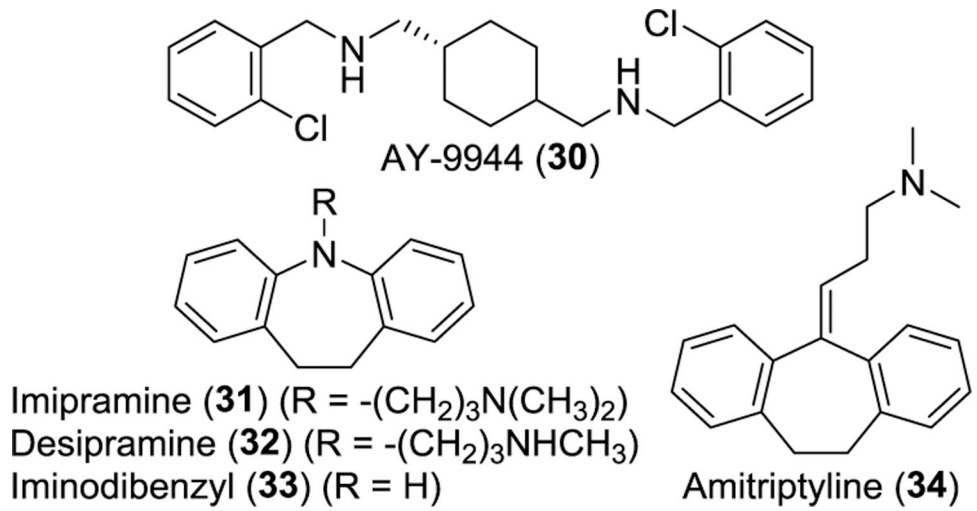

Figure 11.
Structures of representative functional inhibitors of aSMase (FIASMAs).

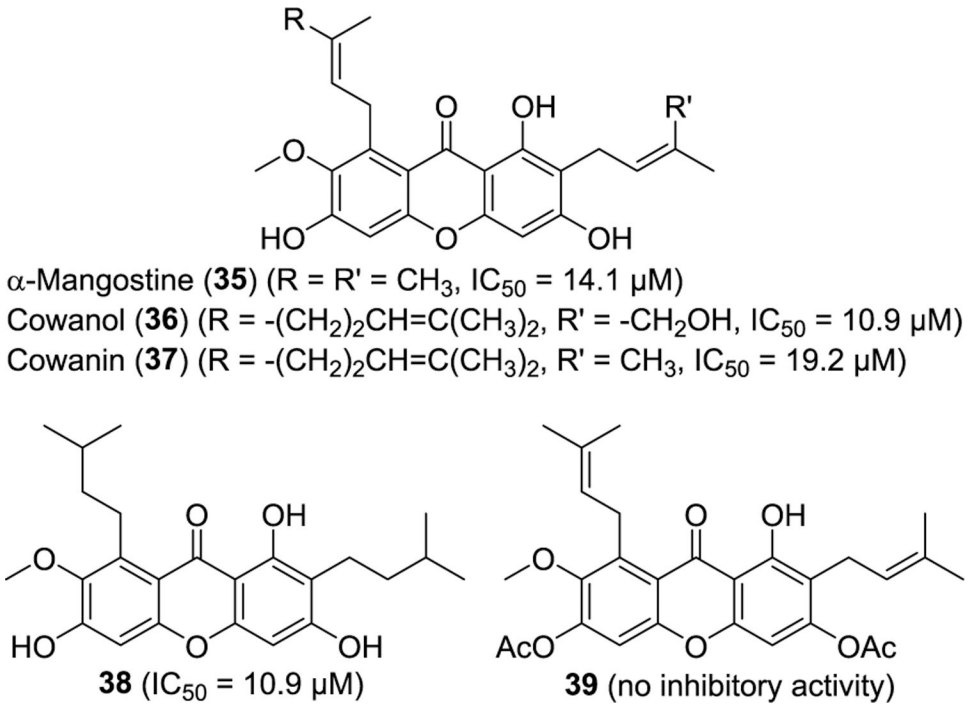

Figure 12.
Structures of xanthone-based aSMase inhibitors **35–39**.

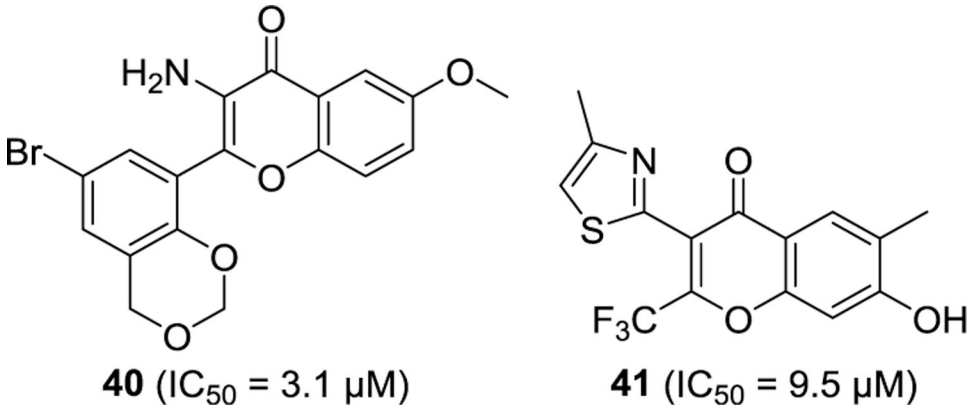

Figure 13.
Structures of γ-pyrone-based aSMase inhibitors **40** and **41**.

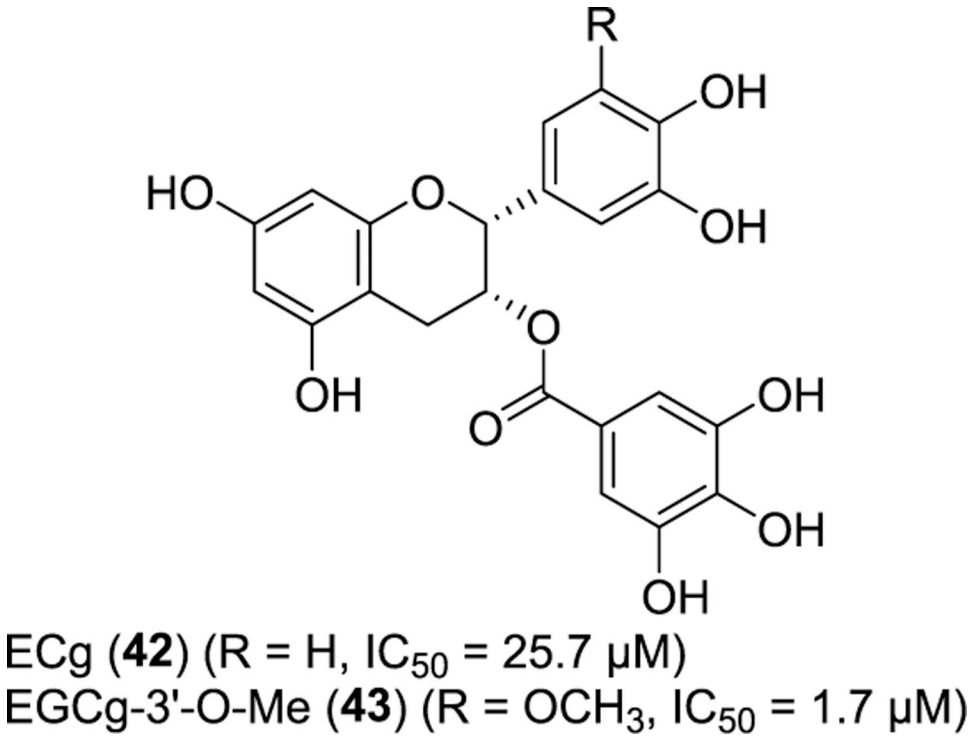

Figure 14.
Structures of catechin-based secretory SMase inhibitors **42** and **43**.

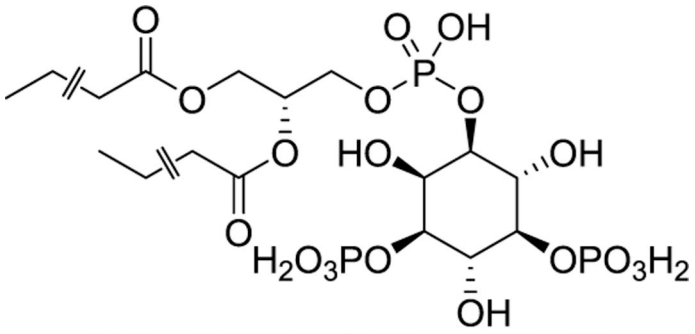

PtdIns3,5P2 (**44**) (K_i = 0.53 μM)

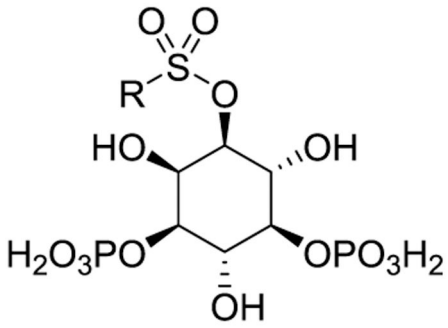

45 (R = CH_3, IC_{50} >100 μM)
46 (R = C_2H_5, IC_{50} >100 μM)
47 (R = C_6H_{13}, IC_{50} = 43 μM)
48 (R = C_8H_{17}, IC_{50} = 4.0 μM)
49 (R = $C_{12}H_{25}$, IC_{50} = 0.9 μM)

Figure 15.
Structures of inositol-4,5-bisphosphate-based aSMase inhibitors **44–49**.

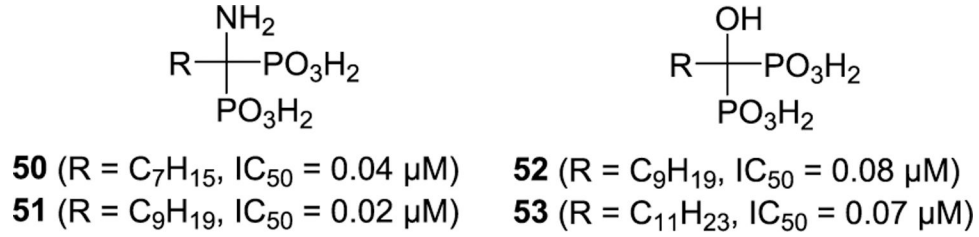

50 (R = C_7H_{15}, IC_{50} = 0.04 μM)
51 (R = C_9H_{19}, IC_{50} = 0.02 μM)
52 (R = C_9H_{19}, IC_{50} = 0.08 μM)
53 (R = $C_{11}H_{23}$, IC_{50} = 0.07 μM)

Figure 16.
Structures of bisphosphonate-based aSMase inhibitors **50–53**.

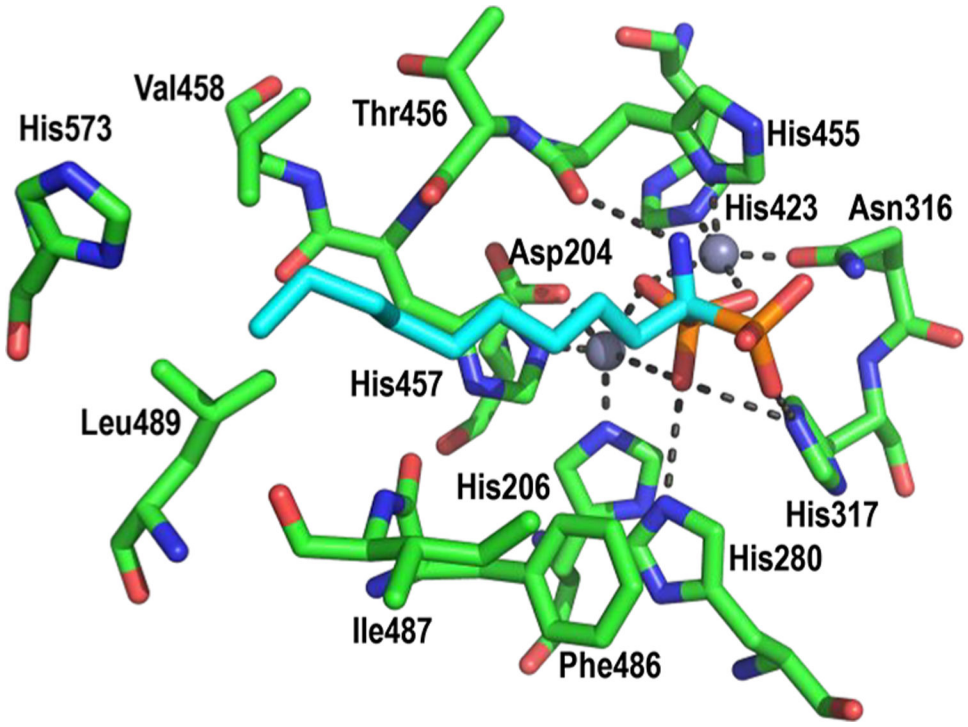

Figure 17.

Crystal structure of the murine aSMase active site in complex with compound **51** (PDB code 5FI9).[66] Key residues are shown as a green stick model, zinc ions are shown as gray spheres, and compound **51** is shown as a cyan stick model.

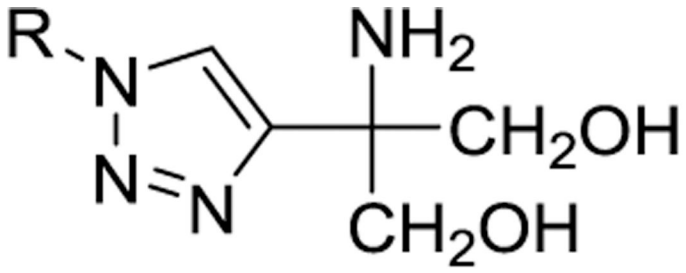

54 (R = C_6H_{13}, IC_{50} = 1.86 μM)
55 (R = C_7H_{15}, IC_{50} = 1.82 μM)
56 (R = C_8H_{17}, IC_{50} = 1.75 μM)
57 (R = C_9H_{19}, IC_{50} = 1.14 μM)

Figure 18.
Structures of serinol-based aSMase inhibitors **54–57**.

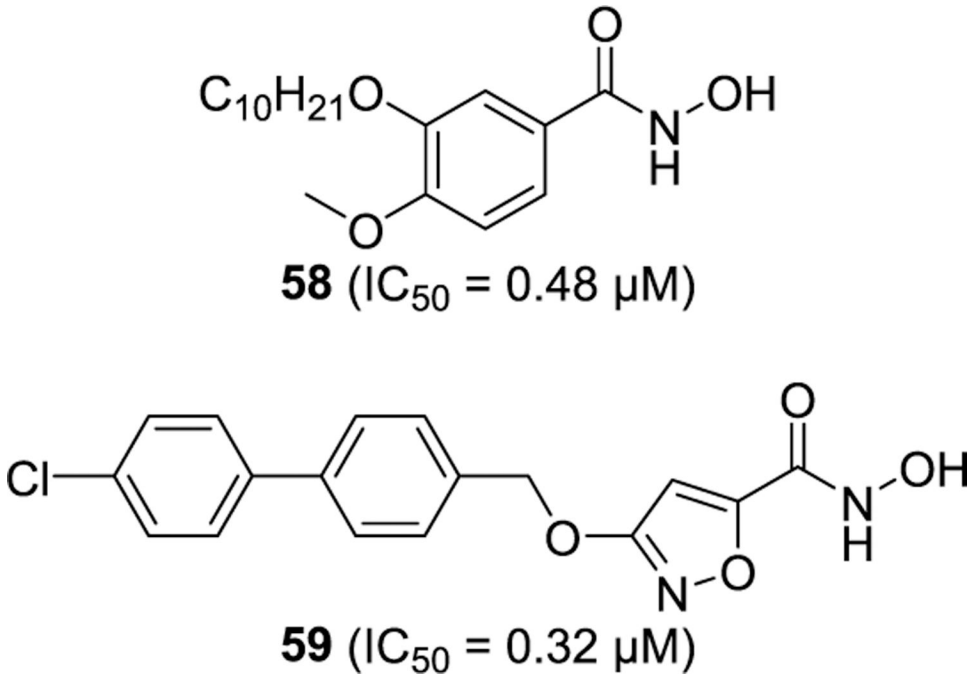

Figure 19.
Structures of hydroxamate-based aSMase inhibitors **58** and **59**.

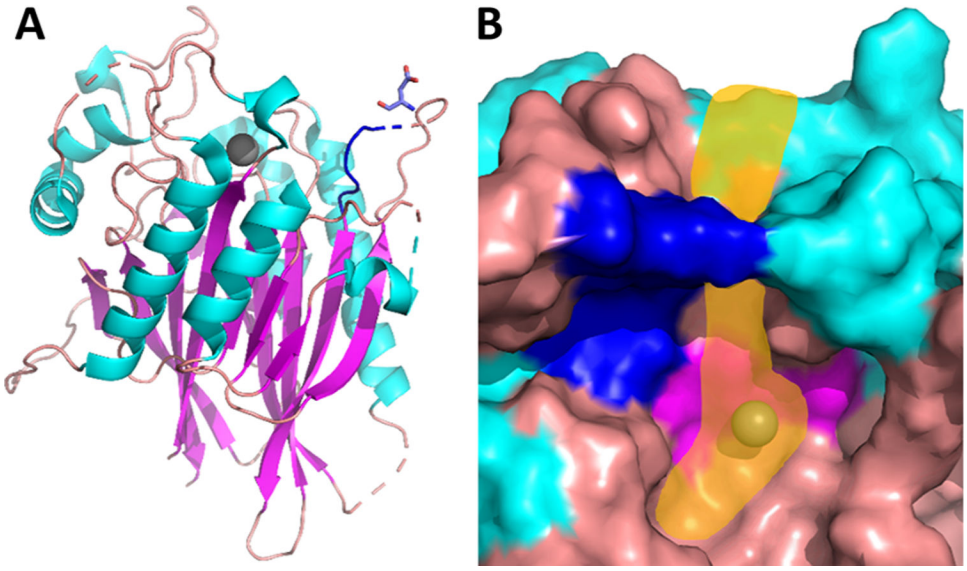

Figure 20.

Crystal structure of human nSMase2 CAT (PDB code 5UVG).[96] (A) Ca^{2+} shown as a gray sphere occupies the position of the primary Mg^{2+} ion required for the Mg^{2+}-dependent activity of nSMase2. DK switch is shown in blue, and the conserved Asp430 is shown as a purple stick model. (B) Close-up view of the substrate binding site. DK switch shown in blue obstructs the entrance to the hydrophobic track stretching from the active site (painted in yellow).

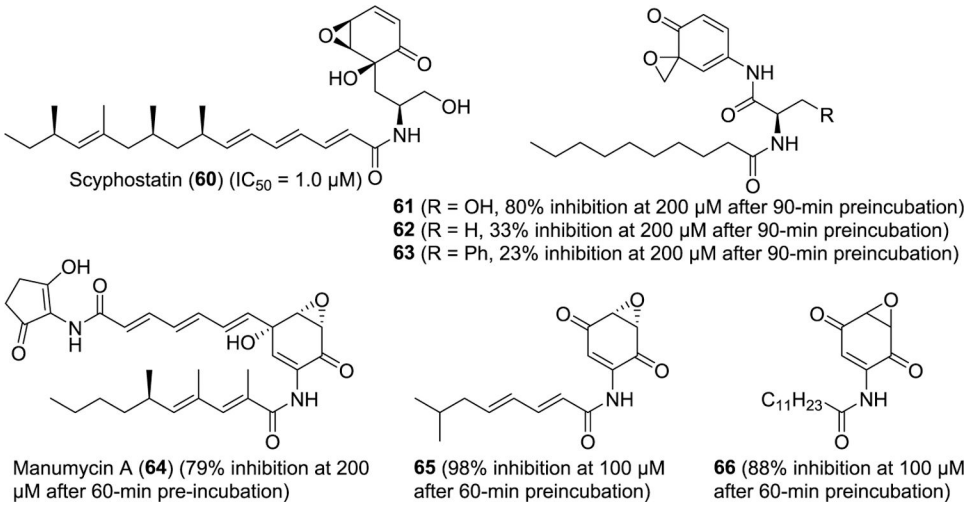

Figure 21.

Structures of scyphostatin **60** and its derivatives **61–66**.

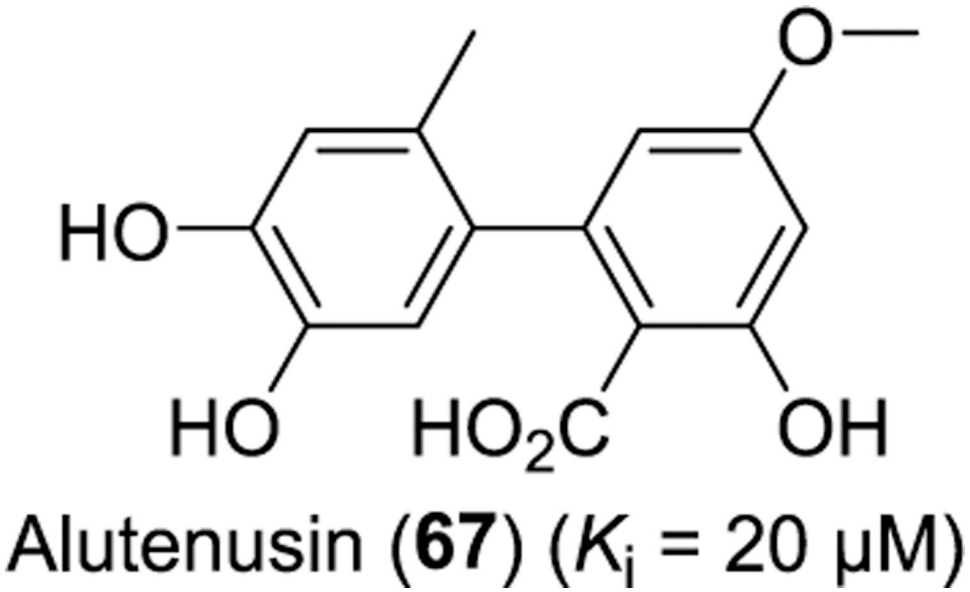

Figure 22.
Structure of alutenusin (**67**).

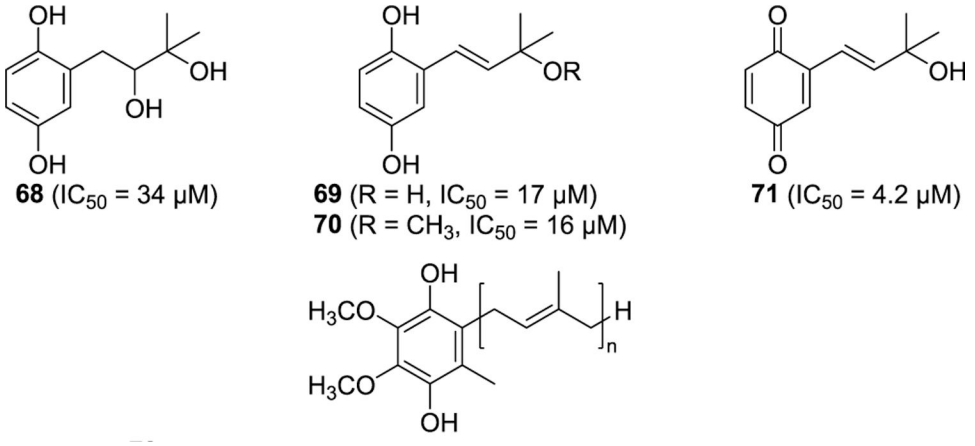

Figure 23.
Structures of benzoquinol- and benzoquinone-based nSMase inhibitors **68–73**.

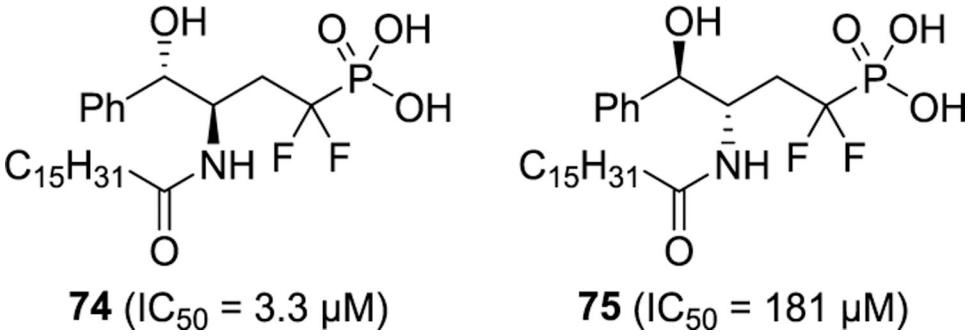

Figure 24.
Structures of phosphonate-based nSMase inhibitors **74** and **75**.

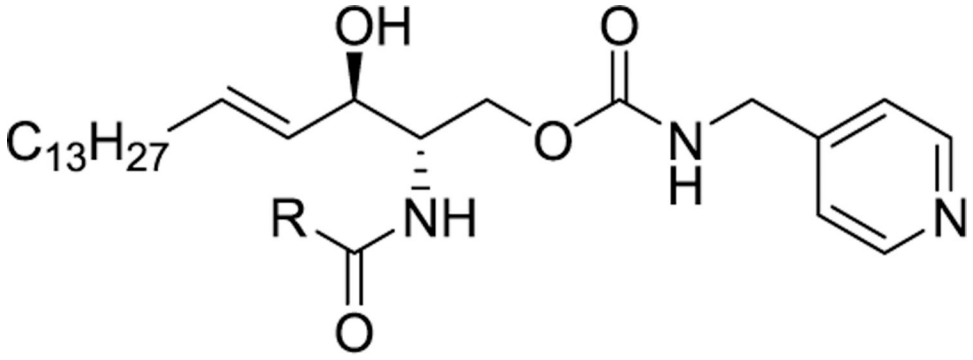

76 (R = *t*-Bu, IC_{50} = 2.8 μM)
77 (R = *i*-Pr, IC_{50} = 1.8 μM)
78 (R = CH_3, IC_{50} > 100 μM)
79 (R = $C_{17}H_{35}$, IC_{50} > 100 μM)

Figure 25.
Structures of carbamate-based nSMase inhibitors **76–79**.

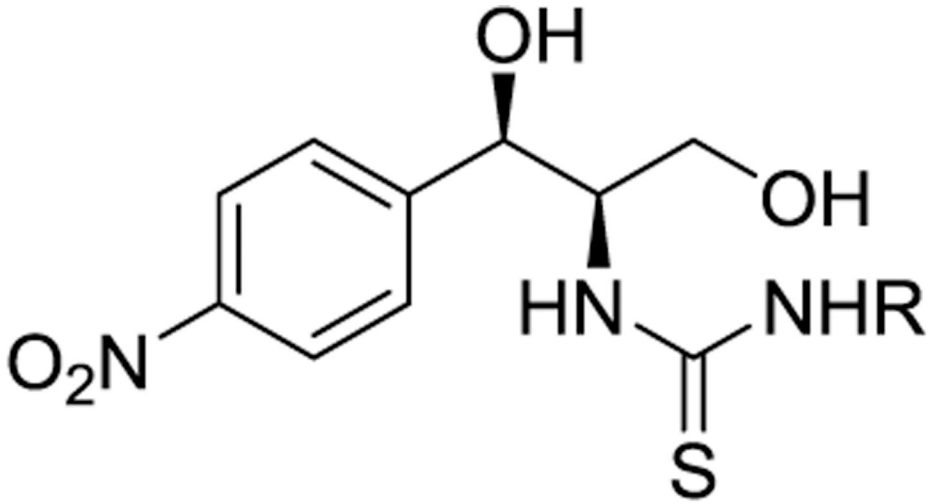

80 (R = $C_{12}H_{25}$, K_i = 1.7 μM)

81 (R = $C_{14}H_{29}$, K_i = 2.5 μM)

Figure 26.
Structures of thiourea-based nSMase inhibitors **80** and **81**.

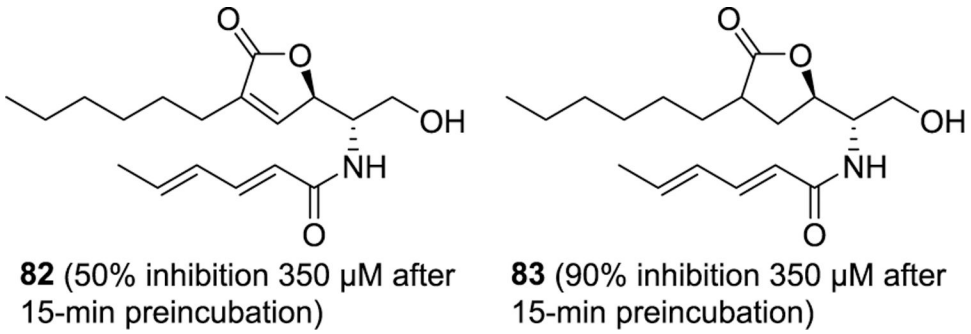

Figure 27.
Structures of γ-lactone-based nSMase inhibitors **82** and **83**.

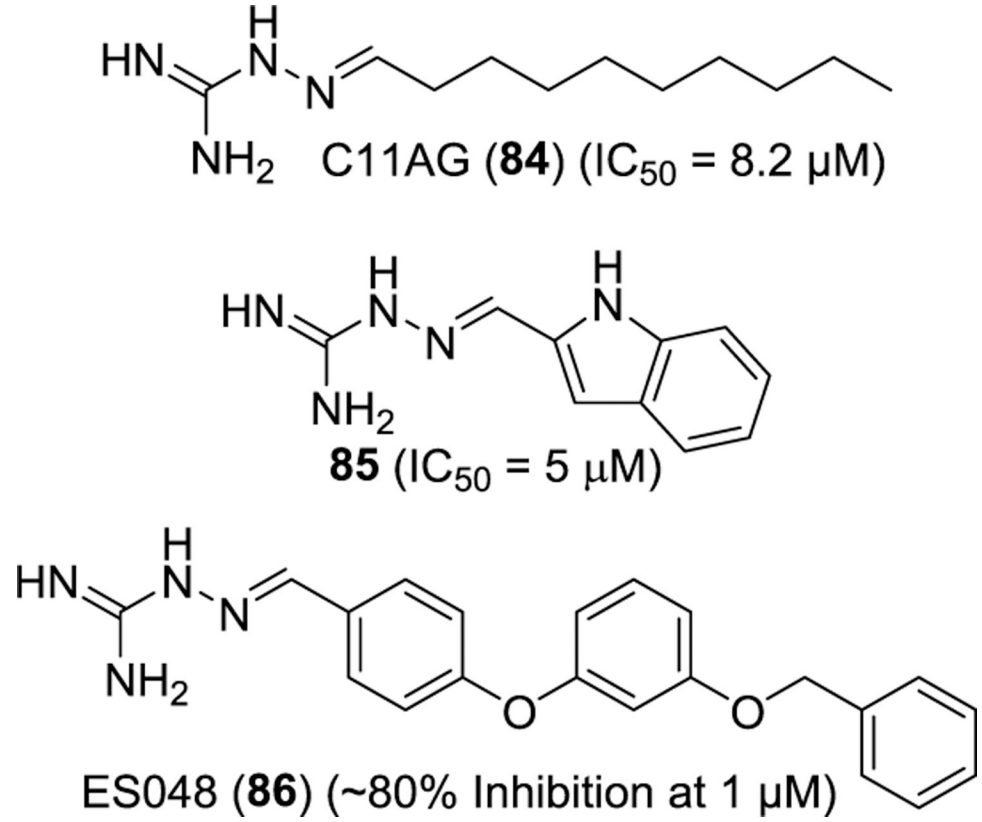

Figure 28.
Structures of aminoguanidine-based nSMase inhibitors **84–86**.

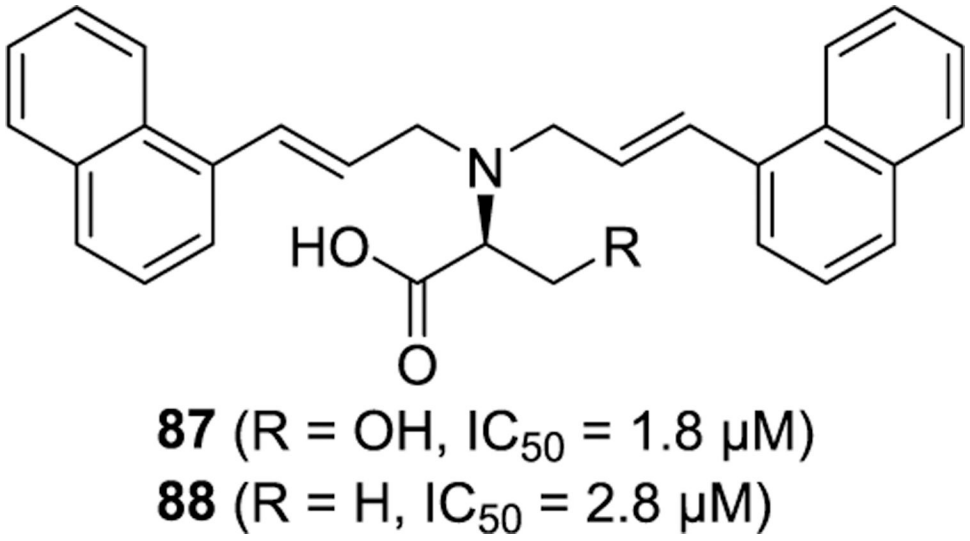

87 (R = OH, IC_{50} = 1.8 μM)
88 (R = H, IC_{50} = 2.8 μM)

Figure 29.
Structures of α-amino acid-based nSMase inhibitors **87** and **88**.

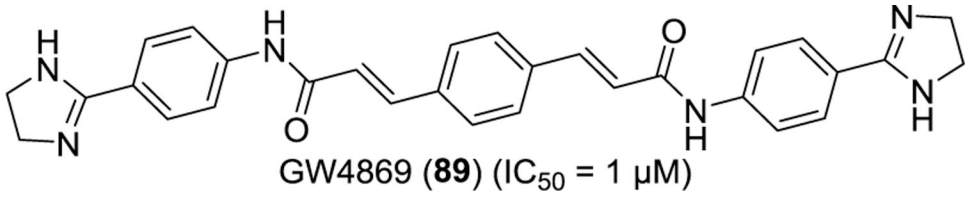

Figure 30.
Structures of GW4869 (**89**).

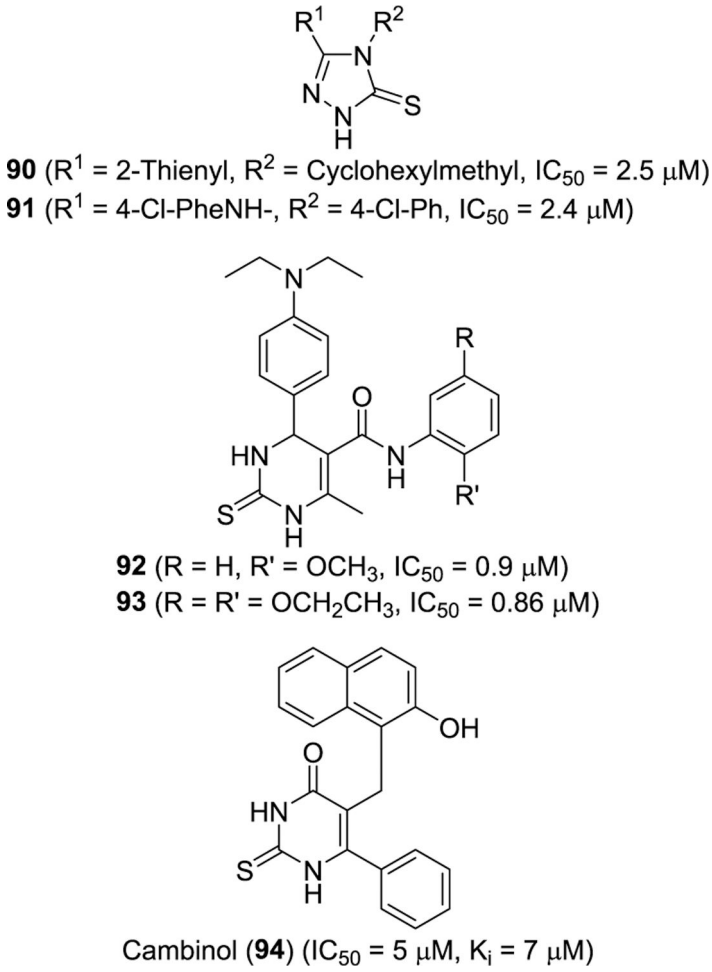

Figure 31.

Structures of nSMase inhibitors **90–94** containing a 1,2,4-triazole-3-thione or pyrimidine-2-thione ring.

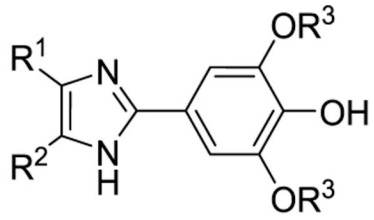

DPTIP (**95**) (R^1 = Ph, R^2 = 2-Thienyl, R^3 = CH_3, IC_{50} = 0.03 μM)
96 (R^1 = R^2 = Ph, R^2 = CH_3, IC_{50} = 0.02 μM)
97 (R^1 = R^2 = 2-Thienyl, R^3 = CH_3, IC_{50} = 0.02 μM)
98 (R^1 = R^2 = Isopropyl, R^3 = CH_3, IC_{50} = 0.07 μM)
99 (R^1 = Ph, R^2 = 2-Thienyl, R^3 = CH_2CH_3, IC_{50} = 0.01 μM)

Figure 32.
Structures of nSMase inhibitors **95–99** based on the 4-(1*H*-imidazol-2-yl)-2,6-dialkoxyphenol scaffold.

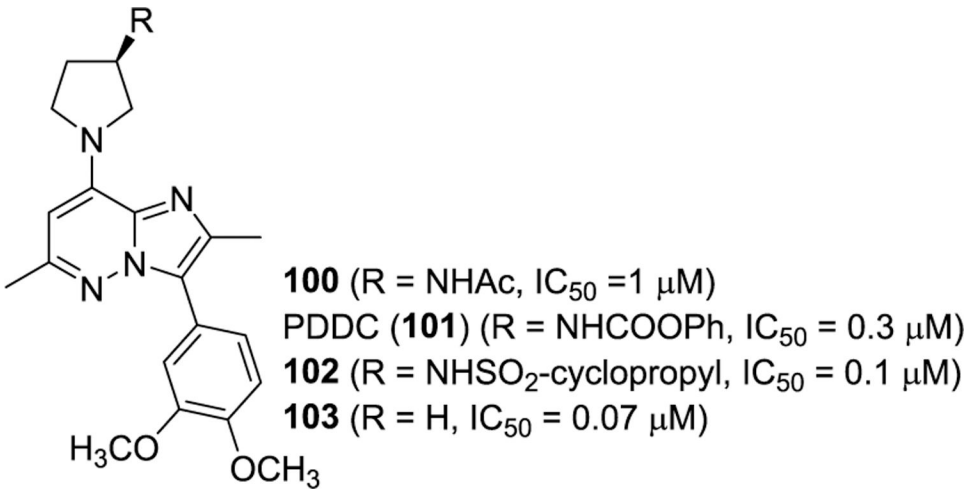

Figure 33.
Structures of nSMase inhibitors **100–103** containing an imidazo[1,2-*b*]pyridazine ring.

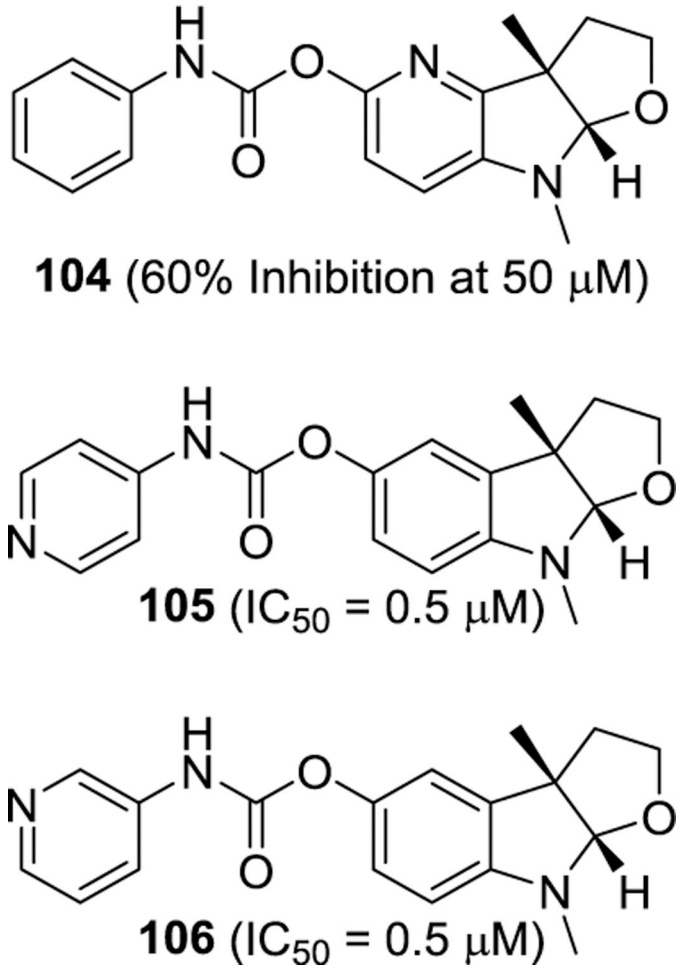

Figure 34.
Structures of phensvenine-based nSMase inhibitors **104–106**.

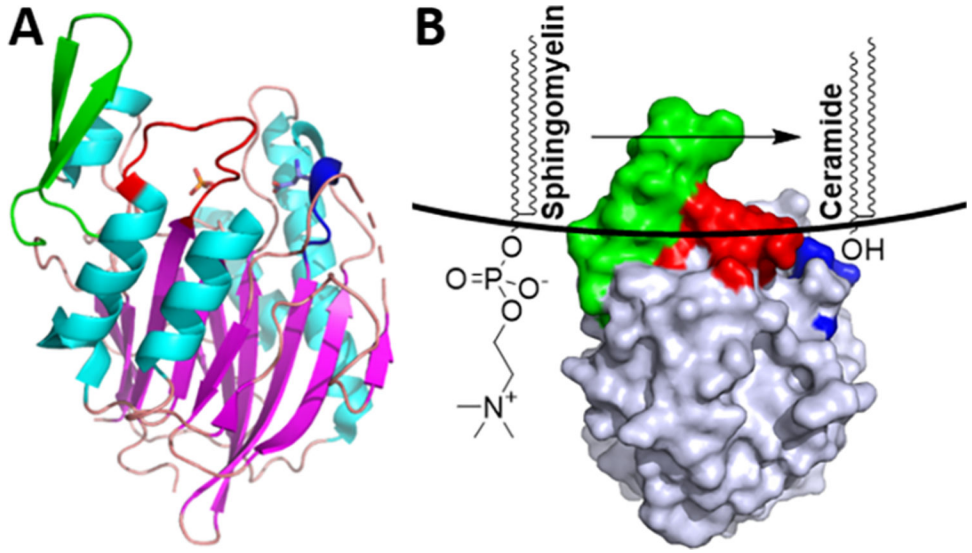

Figure 35.

(A) Overall structure of SmcL (PDB code 1ZWX).[142] The hydrophobic β-hairpin and the hydrophobic loop are shown in green and red, respectively. Phosphate ion shown as an orange/red stick model is likely located in the position occupied by the phosphate moiety of sphingomyelin in the enzyme–substrate complex. DK switch shown in blue forms a short α-helix and directs the conserved Asp160 residue shown as a purple stick model into the active site. (B) Schematic diagram of SmcL-catalyzed hydrolysis of sphingomyelin into ceramide on the outer leaflet of the plasma membrane (adapted from ref 142).

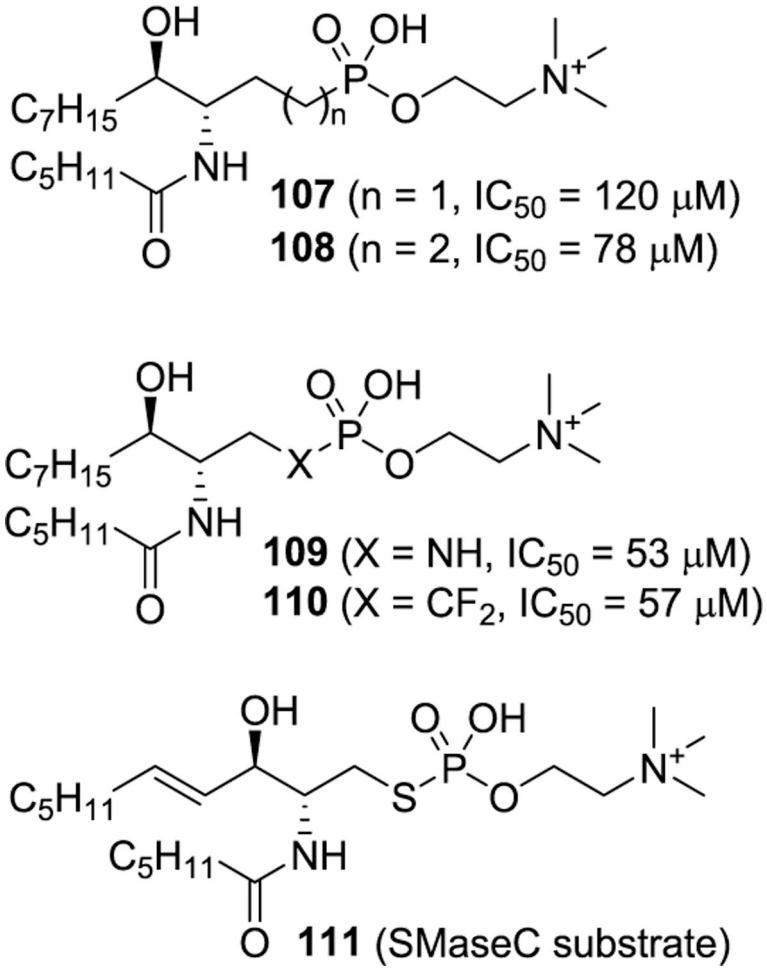

Figure 36.
Structures of phosphorus-based SMaseC inhibitors **107–111**.

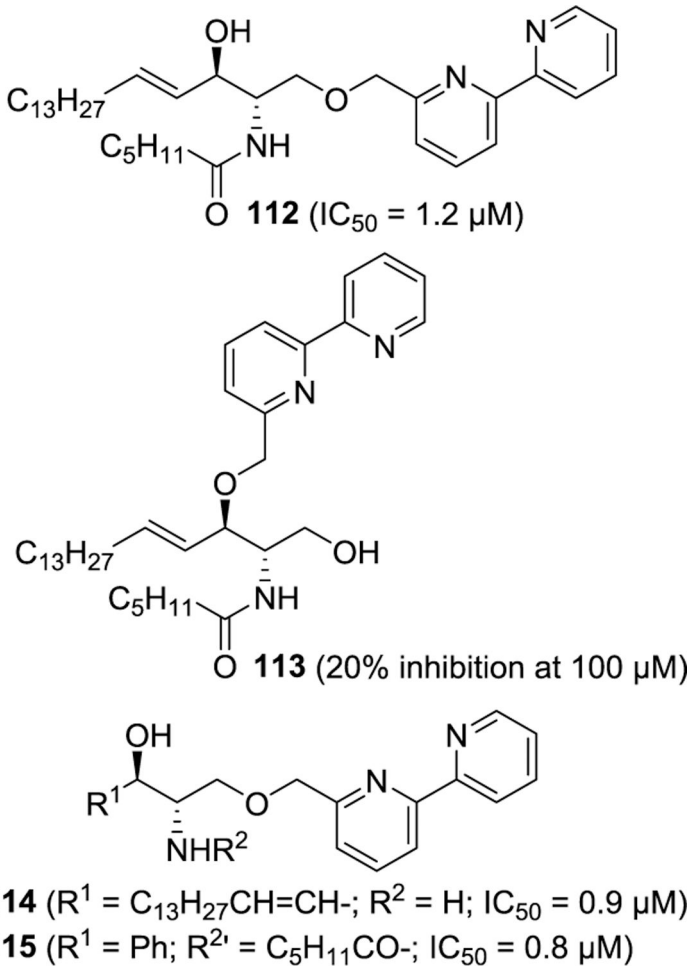

Figure 37.
Structures of SMaseC inhibitors **112–115** containing a bipyridyl moiety.

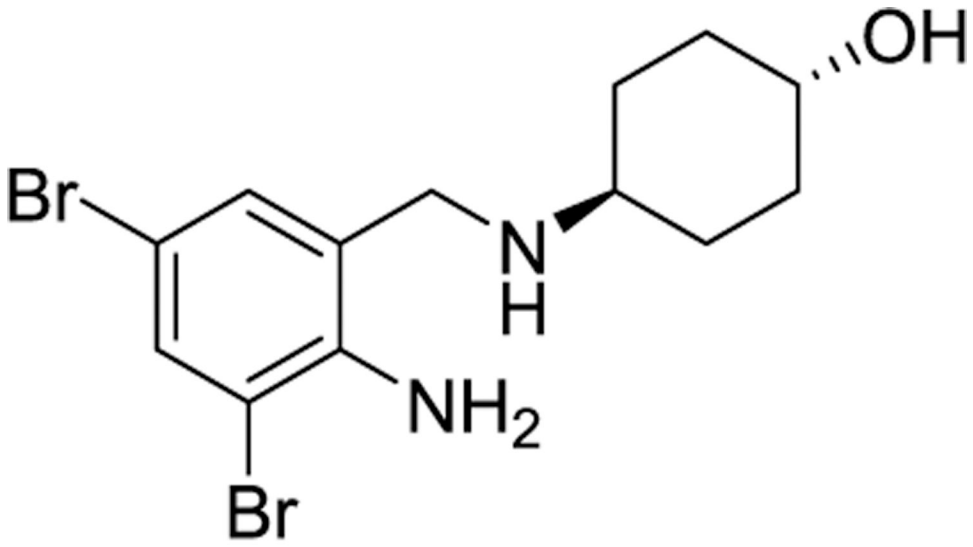

Ambroxol (**116**)
(IC_{50} = 8.1 μM at pH 6.7)
(IC_{50} = 31 μM at pH 5.6)
(IC_{50} > 1100 μM at pH 4.3)

Figure 38.
Structure of a pH-dependent glucocerebrosidase inhibitor, ambroxol **116**.

Table 1.

Representative Inhibitors of Ceramide Biosynthesis

compd	target, *additional known target	pharmacokinetics	preliminary *in vivo* findings
SKI II (**8**)[39,41]	DES1 (K_i = 0.3 μM in HGC-27 cell lysates), *SK1/SK2	Orally available in mice	Showed a significant inhibition of tumor growth in mice bearing JC tumors following oral admin.
P053 (**29**)[60]	CerS1 (IC_{50} = 0.54 μM against human CerS1)	Orally available in mice	Increased fatty acid oxidation in skeletal muscle and reduced overall adiposity in mice fed a high-fat diet following oral admin.
59[89]	aSMase (IC_{50} = 0.32 μM in Huh7 cell lysates)	Distributed to the brain in rats (ip admin)	Improved depression-like behaviors of rats, reduced the cortical and hippocampal aSMase activity, and restored neurogenesis in the brain following ip admin.
DPTIP (**95**)[135]	nSMase2 (IC_{50} = 0.03 μM against human nSMase2)	Distributed to the brain in rats (ip admin)	Attenuated IL-1β-induced ADEV release in in GFAP-GFP mice following ip admin.
PDDC (**101**)[137,138]	nSMase2 (IC_{50} = 0.3 μM against human nSMase2)	Distributed to the brain in rats (oral admin)	Attenuated IL-1β-induced ADEV release in GFAP-GFP mice following oral admin and reversed cognitive impairment in 5XFAD mice following ip admin.
106[139]	nSMase2 (IC_{50} = 0.5 μM against human nSMase2), *AChE	Distributed to the brain (sc admin)	Diminished IL1β-induced brain EV release in tau P301S (line PS19) mice following sc admin.